

### **Response to anonymous referee #3**

**Main comments:** The authors present 2 methods for calculating the  $\kappa$  aerosol hygroscopicity parameter: from 1) Mie calculations that use the aerosol dry size distribution, BC mass concentration and the aerosol scattering hygroscopic growth (fRH) and 2) aerosol size-dependent hygroscopic growth, gRH. The authors use an empirical relationship between the fRH fit parameter, the scattering Angstrom exponent and the ratio fit values from fRH : method 1 kappa fit to create a look up table to predict kappa values.

The paper needs revision to better organize the paper, clarify the different hygroscopic fit calculations as well as discuss differences between the three kappa values.

In general: Break down run-on sentences into two or more sentences. Remove irrelevant information and words. Try not to repeat information. Reduce use of expressions such as “although, therefore, however, widely, especially and traditionally” as these terms usually don’t carry meaning and make the paper more difficult to read. Try to use precise words rather than generalities.

**Response:** Thanks for your comment. We have revised the manuscript according to your suggestions.

### **Specific comments**

**Comment:** Lines 38-42: rewrite as “...,water usually constitutes half of the aerosol mass at a relative humidity of 80% with substantially higher water mass fractions existing at RH values above 90% for most ambient aerosol (Bian et al.,2014). The water content of aerosol and cloud droplets depends on both the ambient RH and hygroscopicity of the aerosol chemical constituents.”

**Response:** Thanks for your comment. We have revised the manuscript accordingly.

**Comment:** rewrite as “ In order to account for the mixed organic and inorganic composition of ambient aerosol Petters and Kriedweiss (2007) proposed a modified version of Kohler theory called  $\kappa$ -Kohler theory to describe a single aerosol hygroscopic growth parameter,  $\kappa$ . The  $\kappa$ -Kohler equation, expressed in terms of the diameter growth factor,  $g(\text{RH})$ , is given in equation 1 below.”

**Response:** Thanks for your suggestion. We revised the manuscript accordingly.

**Comment:** Equation 1: Please change “S” to RH/100. “S” is associated with droplet activation and

may confuse readers. Remove “g” from the equation as it doesn’t belong

**Response:** Thanks for your comment. We revised the manuscript accordingly.

**Comment:** Line 58: remove sentence “In recent ten years, this....” as it states the obvious and doesn’t add to the paper.

**Response:** Thanks for your suggestion. We revised the manuscript accordingly.

**Comment:** Line 71: rewrite as “ The Humidified Tandem Differential Mobility Analyzer (HTDMA) measures the aerosol diameter hygroscopic growth as a function of RH.

**Response:** Thanks for your suggestion. We revised the manuscript accordingly.

**Comment:** Page 3: Remove reference to CCN measurements as it adds confusion and detracts from the discussion of diameter hygroscopic growth.

**Response:** Thanks for your comment. We revised the manuscript accordingly.

**Comment:** Line 84: Remove the Brock et al. reference as he uses a cavity ring down spectrometer and not a nephelometer.

**Response:** Thanks for your comment. We revised the manuscript accordingly.

**Comment:** Line 87-89: Rewrite as “The scattering enhancement factor  $f(RH)$ , defined as  $f(RH) = \sigma_{sp}(RH, \lambda) / \sigma_{sp}(dry, \lambda)$ , characterizes changes in the aerosol scattering coefficient with RH.

**Response:** Thanks for your comment. We revised the manuscript accordingly.

**Comment:** Line 92: Break into 2 sentences and rewrite as “Thus,  $\kappa$  calculated from  $f(RH)$  measurements represents an optically weighted aerosol hygroscopic growth.

**Response:** Thanks for your comment. We revised the manuscript accordingly.

**Comment:** Line 95-99: Don’t start a new paragraph. Rewrite as “Traditionally, derivation of  $\kappa$  from  $f(RH)$  measurements requires aerosol PNSD as well as black carbon (BC) measurements to determine the imaginary part of the refractive index. As PNSD and BC measurements are expensive their

availability in field campaigns are limited.

**Response:** Thanks for your suggestion. We revised the manuscript accordingly.

**Comment:** Clearly identify the 3 methods you use to determine  $\kappa$  by identifying them as Method 1, Method 2 and Method 3. Line 99: Start a new paragraph. “In this paper we use measurements from .... to derive  $\kappa$  values using 3 methods. The first 2 methods derive  $\kappa$  from aerosol diameter hygroscopic growth and the third method derives an aerosol optical parameterization of  $\kappa$ . Method 1, labeled as  $\kappa_{f(RH)}$ , derives  $\kappa$  from aerosol PNSD, BC and nephelometer  $f(RH)$  measurements. Method 2, defined as  $\kappa_{250}$ , derives  $\kappa$  from aerosol diameter hygroscopic growth measurements,  $g(RH)$ , using a High-Humidity Differential Mobility Analyzer (HH-TDMA). Method 3, defined as  $\kappa_{sca}$ , is an empirical determination of  $\kappa$  using only nephelometer measurements of the aerosol scattering coefficient as a function of RH”.

Start a new paragraph to describe how you combine  $\kappa$  values from Methods 1 and 3 to devise a method to predict size-related  $\kappa$  values using only  $f(RH)$  scattering measurements. You need to clearly identify and separate these 3 methods in the paper. Using the terms “Method 1, Method 2 and Method 3” or something similar will clarify and simplify much of the paper discussion.

**Response:** Thanks for your comment. We revised the manuscript accordingly.

**Comment:** You need to describe the nephelometer  $f(RH)$  measurements. What was the RH range and did the instruments operated in parallel or in series? Describe the position of the RH sensors, the type of RH sensor and its uncertainty. How was the RH inside the nephelometer determined? Did the humidifier scan the hydration or dehydration branch of the aerosol RH growth? What range of RH values were used in calculating the fits?

**Response:** Thanks for your comment. We have added these information in the Section 2 of the revised manuscript.

**Comment:** Why are the HTDMA measurements done at such a high RH? At RH values  $>90\%$ , most RH sensors have an uncertainty  $\pm 3\%$  or more. At high RH values the aerosol growth curve is particularly steep such that even a small error in RH would lead to a very high error in  $g(RH)$ . What

not measure  $g(RH)$  at a lower RH such as 80-85%? What is the uncertainty in  $g(RH)$  at 98% ?

**Response:** Thanks for your comment. The basic principle of HH-TDMA is similar to that of HTDMA, however, its special feature is capable of operating stably under extremely high RH conditions (Hennig et al., 2005). The reason that this system operates at RH of 98% is the scientific focus of this instrument during this field campaign is hygroscopic properties of aerosol particles under extremely high RH conditions. Details about the uncertainties of RH and  $g(RH)$  please refer to Hennig et al. (2005).

**Comment:** Line 172: Remove the first two sentences of section 3.2. Accurate measurement of  $f(RH)$  depends on the uncertainty in aerosol scattering and RH. The empirical relationship of scattering to RH isn't difficult to measure or describe. What's difficult is modeling the size-dependent chemical composition of the aerosol, not the measurement itself. Page 7, line 187: Remove the sentence " Here, we give ..." As you haven't described curvature effects and these effects aren't apparent for equation 3, you should remove the sentence.

**Response:** Thanks for your comment. We have revise the manuscript accordingly.

**Comment:** Line 189-198: Simplify the wording.

**Response:** Thanks for your comment. We have revised the manuscript.

**Comment:** One assumption of the  $f(RH)$  kappa parameterization is that  $f_{RH=1}$  at  $RH=0$ . However,  $f(RH)$  values are near constant for  $RH < 40\%$ , meaning  $f(RH)=1$  at  $RH \sim 40$ . What this means is that the fits can't be forced through 1 at  $RH=0$ . The actual equation should be  $f(RH) = b + \kappa(RH/100-RH)$ . Equation 3 doesn't account for aerosol losses in the humidifier and nephelometer. These losses won't affect the gamma fit parameter in equation 2 (provided losses are a percent of the scattering), but will affect determination of  $\kappa$  in equation 3. For example a 10% aerosol loss will change  $\kappa$  by 10%, but multiplying equation 2 by this same 10% loss correction or 1.1 won't change gamma.

**Response:** Thanks for your comment. We agree with the referee that the humidified nephelometer system have the problem of aerosol losses in the humidifier. During Gucheng campaign (introduced in the revised manuscript), the control software of this system will let the humidifier do not humidify the sample air every two days and the period last about two hours. The purpose of doing so is to check the consistency of two nephelometers (Dry nephelometer and Wet Nephelometer). The results are shown

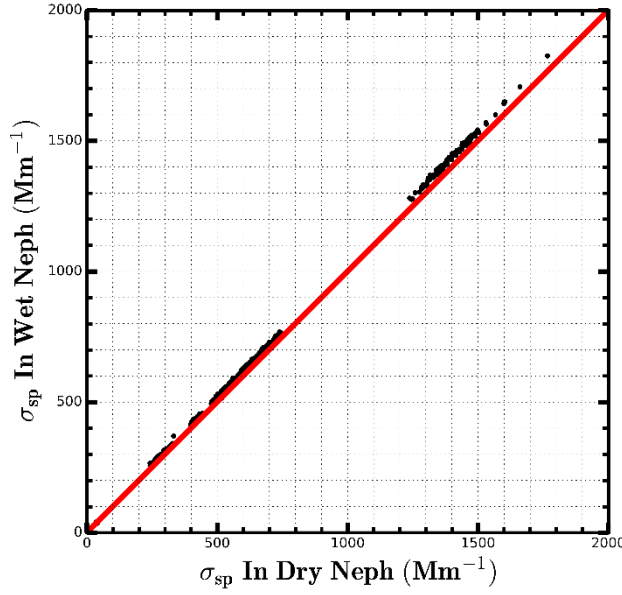


**Figure 1.** x-axis represents  $\sigma_{sp}$  at 525 nm measured by the dry nephelometer, y-axis represents  $\sigma_{sp}$  at 525 nm measured by the wet nephelometer, the red line is 1:1 line.

in Fig.1. The results demonstrate that  $\sigma_{sp}$  measured by the wet nephelometer is slightly higher than that measured by the dry nephelometer, the average relative difference is 3%. The reason that the higher  $\sigma_{sp}$  measured by the wet nephelometer might be attributed to the difference of RH in the dry nephelometer (about 8%) and wet nephelometer (about 15%). In addition, the relative difference between them is within the measurement uncertainty of nephelometer (Müller et al., 2011). This result indicates that aerosol losses in the humidifier have negligible influence on the  $\sigma_{sp}$ .

During processes of measuring  $f(RH)$ , the sample RH in the dry nephelometer ( $RH_0$ ) is not zero. We have modified the fitting formula of measured  $f(RH)$ . According to equation (3) of the manuscript, the measured  $f(RH)_{measure} = \frac{f(RH)}{f(RH_0)}$  should be fitted using the following formula:

$$f(RH)_{measure} = (1 + \kappa_{sca} \frac{RH}{100-RH}) / (1 + \kappa_{sca} \frac{RH_0}{100-RH_0}) \quad (4)$$

And in the revised manuscript, this equation is used for calculating  $\kappa_{sca}$ .

**Comment:** The gamma and kappa fit parameters are sensitive to the RH range of the fit. What range of RH was used in the fits? Note that RH values <40% and >90% will increase error in the fit as the growth curves don't conform to equations 2 or 3 in these RH regions.

**Response:** Thanks for your comment. We have added the information about RH range used in the retrieval algorithm in the revised manuscript. About 50% to 90% for cycles without deliquescence,

about 70% to 90% for cycles with deliquescence.

**Comment:** Line 225-226: rewrite: During deliquescence  $f(RH)$  exhibits an abrupt increase between RH values of 60-65%. As such, only  $f(RH)$  data points with  $RH > 70\%$  were used in determination of  $\kappa$  when deliquescence was apparent.

**Response:** Thanks for your comment. We revised the manuscript accordingly.

**Comment:** Lines 237-240. Be more specific and describe the hygroscopic growth behavior during polluted times more quantitatively. What range of  $\sigma_{sp}$  values were categorized as polluted? Figure 1 shows that  $\sigma_{sp}$  was above 100  $Mm^{-1}$  most of the measurement period. Can you show a plot of  $f(RH)$  vs  $\sigma_{sp}$ ? Can you account for changes in  $f(RH)$  with aerosol loading? How does aerosol size and absorption change with loading?

**Response:** Thanks for your comment. Periods with  $\sigma_{sp} > 100 Mm^{-1}$  are categorized as polluted.

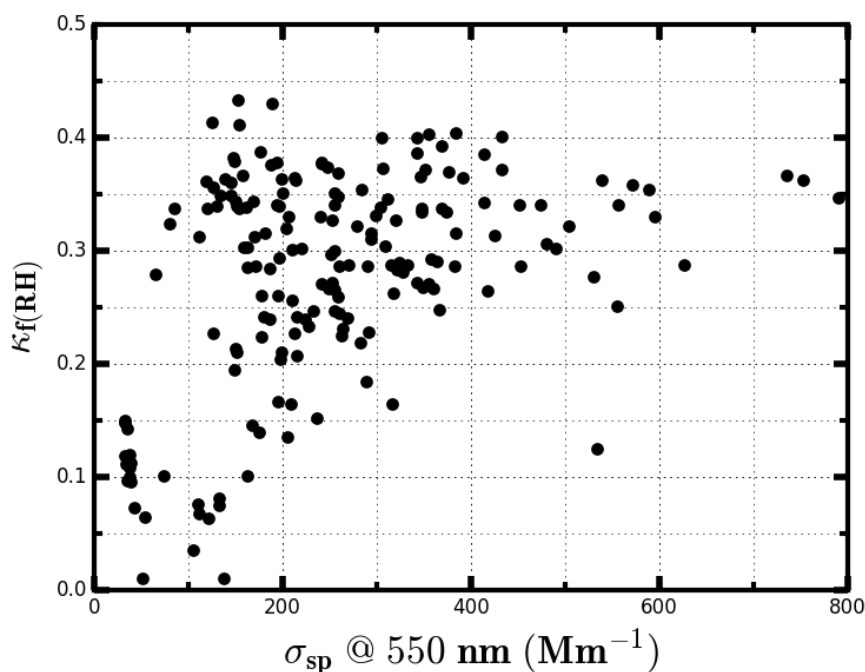


Figure 2. x-axis represents  $\sigma_{sp}$  @ 550 nm, y-axis represents retrieved  $\kappa_f(RH)$ .

During Wangdu campaign, the plot of  $\kappa_f(RH)$  vs  $\sigma_{sp}$  is shown in Fig.2. The aerosol size and absorption changes with aerosol loading is a good scientific topic. Studies of aerosol size changes with aerosol loading can be found in previous studies, such as Shen et al. (2015). The absorption change with aerosol loading is highly variable in polluted region due to complicated emissions and aging

processes. Issues about aerosol size and absorption changes with loading are beyond the scope of this paper.

**Comment:** Line 271: Is  $\kappa_{f(RH)}$  optically weighted or is it a size-dependent  $\kappa$  that is integrated over the entire size distribution? Method 1 varies the size-dependent  $\kappa$  until the Mie calculations equal the scattering  $f(RH)$ . Change “optically weighted” to “size-integrated”.

**Response:** Thanks for your comment. We revised the manuscript accordingly.

**Comment:** Page 10, Lines 266-285: Can you simplify the wording to make this paragraph easier to understand. It would help to distinguish the model  $\kappa$  values from Model 1 and Model 2 if you labeled it  $\kappa_{chem}$

**Response:** Thanks for your comment. We have revised the manuscript.

**Comment:** Page 11, Line 299: A comparison of the kappa and gamma fits to the measured value at a single RH of 85% isn't a good indication of the goodness of fit. Note in Figure 4a that both the gamma and kappa fits are higher than the measured value at 85%. A better indication of the goodness of fit would be a chi-square fit value or the sum of the square of standard deviation of the measured values from the fit line or variance. I suggest replacing Figure 4b with a plot of the probability distribution of the fit variances.

**Response:** Thanks for your comment. We agree with the referee. According to the suggestions of another referee, we have deleted this part.

**Comment:** Lines 313-321: This paragraph is unclear. The co-variance of  $f(RH)$  fit parameters with OMF, SMF and NMF varies with aerosol type; e.g. source and oxidation state or aging. The fit quality depends on the measurement duration as well as the variability in the aerosol type. The chemical information can give an indication of the aerosol hygroscopic growth in the absence of scattering  $f(RH)$  measurements. Gamma and kappa fit values in your comparison are both derived from nephelometer scattering measurements, so they should compare well. Remove the discussion of past comparisons of kappa with aerosol chemical composition

**Response:** Thanks for your comment. We have revised the manuscript accordingly.

**Comment:** Line 338: The ratio  $R_k$  depends on the aerosol size-integrated scattering efficiency. This ratio will vary substantially with the aerosol type and size distribution. The variability of  $R_k$  of this study may not coincide with that of the Brock et al. paper as different aerosol types were sampled under very different conditions. Rewrite sentence as “... the ratio  $\kappa_{sca}/\kappa_{f(RH)}$  may share a similar range of variability.”

**Response:** Thanks for your suggestion. We revised the manuscript accordingly.

**Comment:** Page 13, line 379: replace “PNSD at dry state” with “dry scattering Angstrom exponent”  
Line 380: remove “nevertheless, aerosol hygroscopicity has non-negligible impacts”. The results indicate a strong size-dependence to the hygroscopic growth. Size and hygroscopicity are not separable, nor does one parameter dominate variation in  $R_k$ . Aerosol size would determine or dominate  $R_k$  only if the aerosol chemical composition had no size variation. As sulfate tends to be more prevalent in smaller sizes then  $R_k$  will be larger at higher Angstrom values.

**Response:** Thanks for your suggestion. We have revised the manuscript accordingly.

**Comment:** Lines 378-384: Rewrite this section in terms of variation in the size-dependent chemical composition.

**Response:** Thanks for your comment. We agree with the referee that the size-dependent chemical composition also exerts influence on  $R_k$ . If PNSD is fixed, each size-resolved  $\kappa$  distribution corresponds to a certain  $\kappa_{f(RH)}$ , and  $\kappa_{f(RH)}$  varies within certain range no matter how size-resolved  $\kappa$  distribution changes. Therefore, influences of size-dependent chemical compositions are already included in simulated results of producing the look up table by varying the  $\kappa_{f(RH)}$  from 0 to 0.7 for a fixed aerosol PNSD. This discussion is added in the revised manuscript.

**Comment:** Lines 407-413: Note that the look up table only applies to aerosol on the NCP during the summer and can't be applied to other sites. Aerosol size distributions, secondary processing, and size-dependent composition vary widely with season and region. This method can be used as a tool for



other sites, however it requires measurements of nephelometer scattering, aerosol BC and particle number size distributions.

**Response:** Thanks for your comment. We agree with the referee that aerosol size distributions, secondary processing, and size-dependent composition vary widely with season and region. However, in the simulating processes of producing the look up table, no information about size dependent chemical composition is involved. The look up shown in Fig.6a of the manuscript is produced from measurements of four field campaigns (datasets from a new campaign are added) which were conducted at different seasons and sites. The small variation of  $R_k$  under different Angstrom exponent and  $\kappa_{sca}$  conditions shown in Fig.6b demonstrate good consistency exists between  $R_k$  produced from PNSD and BC measurements of these campaigns. In addition, in the revised manuscript, we have verified this method with datasets obtained from two sites of the NCP in different seasons. Please refer to Fig.7 and Fig.8 of the revised manuscript for more details. The results demonstrate that the look up table is applicable in different sites and seasons.

## Response to anonymous referee #2

**General comment:** If the focus of the manuscript, as stated in the title, is the presentation of a novel method they need to pay more attention to the explanation of the method itself and the validation of the method using additional data (ideally from different measurement sites) and quantify the uncertainties of using the look-up-table to retrieve aerosol hygroscopicity. Otherwise, the authors are just presenting relationships between variables but not actually a new (usable) method. There are many redundancies in the paper that should be omitted as well as typos and grammar spelling errors. Split sentences into two or more individual sentences to improve readability.

**Response:** Thanks for your comment. We agree with the reviewer. In the revised manuscript, the look up table is produced based on PNSD and BC measurements from four different field campaigns. Meanwhile, datasets about PNSD and BC during Wangdu campaign when measurements from the humidified nephelometer system are available are not used in simulating the look up table. In addition, datasets from a different field campaign which is conducted at another site on the NCP in autumn is also used to validate the proposed method. That is, the produced look up table is verified with measurements from two different sites in different seasons. Please refer to Fig.7 and Fig.8 of the revised manuscript for more details. The results demonstrate that the look up table is applicable in different sites and seasons. As to uncertainties of  $R_k$  under different Angstrom exponent and  $\kappa_{sca}$  conditions, the standard deviations of  $R_k$  within each grid of the look up table are shown in Fig.6b.

## Specific comments

**Comment:** Line21: avoid redundancies like “newly proposed novel approach”

**Response:** Thanks for your suggestion. We revised the manuscript accordingly.

**Comment:** Line22: Replace by “ . . . is that  $\kappa_{f(RH)}$  can be estimated without any additional information...”

**Response:** Thanks for your suggestion. We revised the manuscript accordingly.

**Comment:** Line34: “. . .most important factors affecting these . . .” Introduction: there are too much methodological information in the introduction, that should be moved to the methodology section.

**Response:** Thanks for your suggestion. This sentence reflects the significance of aerosol

hygroscopicity, and this is the motivation of this research.

**Comment:** Line104: “similar to”

**Response:** Thanks for your suggestion. We revised the manuscript accordingly.

**Comment:** Line107: “based on”

**Response:** Thanks for your comment. We revised the manuscript accordingly.

**Comment:** Section2: This section is very bad organized. Include a table with information about the campaigns (dates, sites, data used here from each campaign, etc). What is the time resolution of the PM2.5 filter samples? 24 hours? How often is the sampling performed?

**Response:** Thanks for your suggestion. We revised this section according to your suggestions.

**Comment:** More information on HH-TDMA measurements and inversion routine should be presented. Same applies for the nephelometers tandem. Include information on nephelometers correction and calibration, humidogram schedule, RH range in the dry neph, where were the RH sensors located in the system?, how often were the sensors calibrated?

**Response:** Thanks for your suggestion. We added information about the nephelometer system in Section 2 of the revised manuscript. The instrument set-up of HH-TDMA and inversion routine of  $\kappa$  from measurements of HH-TDMA are introduced in detail in Liu et al. (2011).

**Comment:** Line120: replace dot by comma

**Response:** Thanks for your suggestion. We have revised the manuscript.

**Comment:** Section 3.1: Further details on the methods used to derive the  $\kappa$  parameter should be given even though the methods were published before. At least the basic information to allow the reader to understand the manuscript. Concerning the  $\kappa_{f(RH)}$  method, which chemical species have been considered apart of BC? A table including the chemical species, refractive indices, densities and contribution during the measurement period must be included.

**Response:** Thanks for your comment. The flow chart of retrieving  $\kappa_{f(RH)}$  is provided in the supporting information. A simplified aerosol model was applied to aerosol optical calculations. In the model, aerosol components are divided into two classes in terms of their optical properties: the light absorbing component (BC) and less absorbing components (comprising inorganic salts and acids such as sulfates, nitrates, ammoniums, as well as most of the organic compounds). We have added this statement in Section 3.1 of the revised manuscript.

**Comment:** In the Mie routine, is the chemistry considered as constant during the campaign? See my previous comment on PM2.5 sampling schedule.

**Response:** Thanks for your comment. In this paper, a simplified aerosol model was applied to aerosol optical calculations. In the model, aerosol components are divided into two classes in terms of their optical properties: the light absorbing component (BC) and less absorbing components (comprising inorganic salts and acids such as sulfates, nitrates, ammoniums, as well as most of the organic compounds). We have added this statement in Section 3.1 of the revised manuscript.

**Comment:** Section 3.2: The reference of Quinn et al. (2005) is not appropriate here. The gamma parameterization was first introduced in Kasten (1969) and Hanel (1980). Kasten, F., 1969. Visibility forecast in the phase of pre-condensation. *Tellus* 21 (5), 631-635 Hanel, G., 1980. Technical Note: an attempt to interpret the humidity dependencies of the aerosol extinction and scattering coefficients. *Atmos. Environ.* 15, 403-406.

**Response:** Thanks for your comment. We have revised the reference accordingly.

**Comment:** Line 194: avoid redundancy, this sentence “more details . . .” could be omitted.

**Response:** Thanks for your comment. We have revised the manuscript accordingly.

**Comment:** Results: Line 207-221: This paragraph could be omitted since basically is a repetition of the results presented in Kuang et al., (2016) and does not provide any additional/useful information.

**Response:** Thanks for your comment. We have deleted these sentences.

**Comment:** Line 207: information about nephelometer correction should be moved to the instrument section

**Response:** Thanks for your suggestion. We revised the manuscript accordingly.

**Comment:** Lines 212, 216 and somewhere else: “a lot” is not very scientific, be more quantitative and avoid colloquial expressions.

**Response:** Thanks for your comment. We have revised the manuscript accordingly.

**Comment:** Line 257: This paragraph should be rewritten. What is the aim of including these two additional campaigns?

**Response:** Thanks for your comment. The aim of including PNSD and BC information from different campaigns is to simulate variations of  $R_k$  under different conditions. We have added this sentence in the revised manuscript.

**Comment:** Line 297: “The fitting performance . . . values” could be omitted. Again, avoid redundancy.

**Response:**

**Comment:** Line 300: The  $\gamma$ -Method and  $\kappa$ -Method are just different ways of fitting the experimental  $f(\text{RH})$ -RH relationship. Which method is better or worst depends on your specific data, and many other equations have been previously proposed in the literature (Titos et al., 2016). The discussion in lines 300-306 and figure 4 about which fitting is best do not add much and could be omitted.

**Response:** Thanks for your comment. We have deleted these sentences.

**Comment:** Line 316: “pretty good linear relationship” does not sound very quantitative neither scientific . . . Try to be more specific . . .

**Response:** Thanks for your comment. We have revised the manuscript accordingly.

**Comment:** Line 333: This is the first time that  $\kappa_{\text{chem}}$  and  $\kappa_{\text{ext}}$  are introduced.

**Response:** Thanks for your comment. We revised the manuscript.

**Comment:** Line 347 and somewhere else: Avoid repetitions like “which is introduced in Section

...”

**Response:** Thanks for your comment. We have revised the manuscript accordingly.

**Comment:** Line 359-360: “and then it turns out”, “much more complex” ... this is not very appropriate for a scientific paper...

**Response:** Thanks for your comment. This sentences is revised as the following: “A robust linear relationship is found between  $\kappa_{f(RH)}$  and  $\kappa_{sca}$  in Sect.4.2 , however, results of further analysis suggest that  $R_k$  varies a lot”

**Comment:** References of Titos et al., 2016 and Zieger et al., 2014 are not used appropriately here. The Angstrom exponent was first introduced by Angstrom!

**Response:** Thanks for your comment. We have deleted the reference.

**Comment:** Line 377: Keep in mind that the Angstrom exponent is not a measure of the PNSD, it provides information on mean predominant aerosol size so values close to 2 denote a predominance of fine particles while values below 1 denote a predominance of coarse particles.

**Response:** Thanks for your comment. We have revised the sentence as the following: “Based on results shown on Fig.6a, the different impacts of aerosol hygroscopicity and dry scattering Ångström exponent on  $R_k$  can be distinguished to some extent”.

**Comment:** Line 393 and Figure 7: This comparison exercise is interesting but it is not appropriately done. The predicted  $R_k$  values using the look-up-table are compared with the measured  $R_k$  values. However, these measured  $R_k$  were used before to generate the look-up-table. Thus, it is clear that a high correlation is expected. A different dataset, with additional  $R_k$  values not used to generate the look-up-table should be used for validation of the proposed model. Otherwise, the same data that is used to generate the model is used to validate it, which is meaningless.

**Response:** Thanks for your comment. In the revised manuscript. The dataset about PNSDs and mass concentrations of BC are not used in the processes of produing the look up table shown in Fig.6a. Thus, the look up table is independent of measurements during periods when f(RH) measurements are

available. In addition,  $f(\text{RH})$  measurements from another campaign is also used to verify the manuscript.

**Comment:** If the authors really expect researchers to use their method, they should provide them with an uncertainty range for  $R_k$  as a function of the Angstrom exponent and  $\kappa_{sca}$ . Probably, higher errors are expected at higher  $\kappa_{sca}$  values? This is certainly needed if they expect people to use the look-up-table. In general, the manuscript lacks of an appropriate treatment of errors despite the large expected errors for the hygroscopicity parameters.

**Response:** Thanks for your comment. We agree with the referee. The uncertainty range of  $R_k$  based on the simulative results is shown in Fig.6b. The results is consistent with the referee's point that higher errors are expected at higher  $\kappa_{sca}$  values. The maximum  $\kappa_{sca}$  of the look up table is 0.4, if  $R_k$  is 0.8 (close to the simulated highest  $R_k$  shown in Fig.5b), the corresponding  $f(80\%)$  is 2.6. According to the review of Titos et al. (2016), most of  $f(80\%)$  for continental aerosols are lower than 2.6. This look up table already covers most situations for continental aerosol types.

Hennig, T., Massling, A., Brechtel, F. J., and Wiedensohler, A.: A tandem DMA for highly temperature-stabilized hygroscopic particle growth measurements between 90% and 98% relative humidity, *Journal of Aerosol Science*, 36, 1210-1223, 10.1016/j.jaerosci.2005.01.005, 2005.

Liu, P. F., Zhao, C. S., Göbel, T., Hallbauer, E., Nowak, A., Ran, L., Xu, W. Y., Deng, Z. Z., Ma, N., Mildenberger, K., Henning, S., Stratmann, F., and Wiedensohler, A.: Hygroscopic properties of aerosol particles at high relative humidity and their diurnal variations in the North China Plain, *Atmos. Chem. Phys.*, 11, 3479-3494, 10.5194/acp-11-3479-2011, 2011.

Müller, T., Laborde, M., Kassell, G., and Wiedensohler, A.: Design and performance of a three-wavelength LED-based total scatter and backscatter integrating nephelometer, *Atmos. Meas. Tech.*, 4, 1291-1303, 10.5194/amt-4-1291-2011, 2011.

Shen, X. J., Sun, J. Y., Zhang, X. Y., Zhang, Y. M., Zhang, L., Che, H. C., Ma, Q. L., Yu, X. M., Yue, Y., and Zhang, Y. W.: Characterization of submicron aerosols and effect on visibility during a severe haze-fog episode in Yangtze River Delta, China, *Atmospheric Environment*, 120, 307-316, <http://doi.org/10.1016/j.atmosenv.2015.09.011>, 2015.

Titos, G., Cazorla, A., Zieger, P., Andrews, E., Lyamani, H., Granados-Muñoz, M. J., Olmo, F. J., and Alados-Arboledas, L.: Effect of hygroscopic growth on the aerosol light-scattering coefficient: A review of measurements, techniques and error sources, *Atmospheric Environment*, 141, 494-507, <http://dx.doi.org/10.1016/j.atmosenv.2016.07.021>, 2016.

# A novel method to derive the aerosol hygroscopicity parameter based only on measurements from a humidified nephelometer system

Ye Kuang<sup>1</sup>, ChunSheng Zhao<sup>1</sup>, JiangChuan Tao<sup>1</sup>, YuXuan Bian<sup>2</sup>, Nan Ma<sup>3</sup>, Gang Zhao<sup>1</sup>

[1]{Department of Atmospheric and Oceanic Sciences, School of Physics, Peking University, Beijing, China}

[2]{State Key Laboratory of Severe Weather, Chinese Academy of Meteorological Sciences}

[3]{Leibniz Institute for Tropospheric research, Leipzig, Germany}

\*Correspondence to: C. S. Zhao (zcs@pku.edu.cn)

## Abstract

Aerosol hygroscopicity is crucial for understanding roles of aerosol particles in atmospheric chemistry and aerosol climate effects. Light scattering enhancement factor  $f(RH, \lambda)$  is one of the parameters describing aerosol hygroscopicity which is defined as  $f(RH, \lambda) = \sigma_{sp}(RH, \lambda) / \sigma_{sp}(dry, \lambda)$  where  $\sigma_{sp}(RH, \lambda)$  or  $\sigma_{sp}(dry, \lambda)$  represents  $\sigma_{sp}$  at wavelength  $\lambda$  under certain RH or dry conditions. Traditionally, an overall hygroscopicity parameter  $\kappa$  can be retrieved from measured  $f(RH, \lambda)$ , hereinafter referred to as  $\kappa_{f(RH)}$ , by combining concurrently measured particle number size distribution (PNSD) and mass concentration of black carbon. In this paper, a new method is proposed to directly derive  $\kappa_{f(RH)}$  based only on measurements from a three-wavelength humidified nephelometer system. The advantage of this newly proposed **novel** approach is that **it allows researchers to estimate  $\kappa_{f(RH)}$  can be estimated** without any additional information about PNSD and black carbon. **This method is verified with measurements from two different field campaigns.** Values of  $\kappa_{f(RH)}$  estimated from this new method agree very well with those retrieved by using the traditional method, **all points lie nearby 1:1 line, the average difference between  $\kappa_{f(RH)}$  derived from newly proposed method and traditional method is 0.005 and** the square of correlation coefficient between them is 0.99. **The verification results demonstrate that this newly proposed method of deriving  $\kappa_{f(RH)}$  is applicable in different sites and seasons.**



## 1. Introduction

Atmospheric aerosol particles play vital roles in visibility, energy balance and the hydrological cycle of the Earth-atmosphere system and have attracted a lot of attention in recent decades. Aerosol particles suspended in the atmosphere directly influence radiative transfer of solar radiation and indirectly affect cloud properties, therefore, have large impacts on climate change. Especially, uncertainties in direct aerosol radiative forcing due to anthropogenic aerosols and in aerosol indirect forcing caused by aerosol interaction with clouds contribute most to the total uncertainty in climate forcing (Boucher et al., 2013). One of the most important factors affect these uncertainties is the interaction between aerosol particles and ambient atmospheric water vapour (Zhao et al., 2006; Kuang et al., 2016b). Under supersaturated conditions, aerosol particles serve as cloud condensation nuclei (CCN) and hence influence cloud properties. Under subsaturated conditions, with respect to typical aerosol compositions, liquid water content condensed on aerosol particles usually constitute about half of the total aerosol mass water usually constitutes about half of the aerosol mass at a relative humidity (RH) of 80% with substantially higher water mass fractions existing at RH values above 90% for most ambient aerosol (Bian et al., 2014). Liquid water usually dominates the total aerosol mass in most aerosol types when RH is above 90% (Bian et al., 2014). The amounts of condensed water content of aerosol in ambient aerosols and cloud droplets depend both on both the ambient RH and hygroscopicity of the aerosol chemical constituents water uptake abilities of the aerosol components and ambient RH.

Traditionally, the Köhler theory (Petters and Kreidenweis, 2007) is widely used to describe the hygroscopic growth of aerosol particles and successfully used in laboratory studies for single component and some multicomponent particles. However, it is found that most atmospheric aerosol particles usually consist of both organic and inorganic constituents (Murphy et al., 1998) rather than consist of a single component. Given this, a modified version of Köhler theory called  $\kappa$ -Köhler theory is proposed by Petters and Kreidenweis (2007) and widely used in recent ten years to study the hygroscopic growth of aerosol particles. The formula of this theory is expressed as the following In order to account for the mixed organic and inorganic composition of ambient aerosol, Petters and Kreidenweis (2007) proposed a modified version of Köhler theory called  $\kappa$ -Köhler theory to describe a single aerosol hygroscopic growth parameter,  $\kappa$ . The  $\kappa$ -Köhler equation, expressed in terms of the diameter growth factor,  $g(\text{RH})$ , is given in equation (1) below:

$$\frac{RH}{100} S = \frac{g D^3 - 1 D_d^3}{g D^3 - D_d^3 (1 - \kappa)} \cdot \exp\left(\frac{4 \sigma_{s/a} \cdot M_{water}}{R \cdot T \cdot D_d \cdot \rho_w \cdot g}\right) \quad (1)$$

where ~~S is the saturation ratio, D is the diameter of the droplet~~  $g$  corresponds to  $g(RH)$ ,  $D_d$  is the dry diameter,  $\sigma_{s/a}$  is the surface tension of solution/air interface,  $T$  is the temperature,  $M_{water}$  is the molecular weight of water,  $R$  is the universal gas constant,  $\rho_w$  is the density of water, and  $\kappa$  is the hygroscopicity parameter. This theory is not only applicable to single-component aerosol particles, but also to multicomponent aerosol particles. With regard to a multicomponent aerosol particle, the Zdanovskii, Stokes, and Robinson assumption can be applied. The hygroscopicity parameter  $\kappa$  of multicomponent aerosol particle can be derived by using the following formula:  $\kappa = \sum_i \varepsilon_i \cdot \kappa_i$ , where  $\kappa_i$  and  $\varepsilon_i$  represent the hygroscopic parameter and volume fraction of each component. ~~In recent ten years,~~ This hygroscopicity parameter  $\kappa$  has received much attentions and turns out to be a very effective parameter to study aerosol hygroscopicity. This hygroscopicity parameter  $\kappa$  makes the comparison of the aerosol hygroscopicity at different sites around the world and different time periods more convenient. In addition, hygroscopicity parameter  $\kappa$  also facilitates the intercomparison of aerosol hygroscopicity derived from different techniques and measurements made at different RHs. This hygroscopicity parameter  $\kappa$  is widely used to account the influence of aerosol hygroscopic growth on aerosol optical properties as well as aerosol liquid water contents (Tao et al., 2014; Kuang et al., 2015; Brock et al., 2016; Bian et al., 2014; Zieger et al., 2013) and to examine the role of aerosol hygroscopicity in CCN (Chen et al., 2014; Gunthe et al., 2009; Ervens et al., 2010). ~~Therefore,~~ the derived  $\kappa$  values from field campaigns and laboratory studies will further our understanding in aerosol hygroscopicity and help estimate the influences of aerosol hygroscopic growth on different aspects of atmospheric processes.

~~Currently, several types of instruments are widely used in field campaigns to study the aerosol hygroscopicity through different aspects of aerosol properties.~~ The Humidity Tandem Differential mobility Analyzer (HTDMA) ~~measures the aerosol diameter hygroscopic growth as a function of RH operates below water saturation and directly measures the aerosol hygroscopic growth factor of selected particles which have certain diameters at specified RH points.~~ The aerosol hygroscopicity parameter  $\kappa$  can be directly derived from measurements of HTDMA by applying equation (1) (Liu et al., 2011; Wu et al., 2016). ~~Through relating the aerosol hygroscopicity to CCN properties, measurements of size resolved CCN efficiency spectra can also be used to infer the hygroscopicity~~

parameter  $\kappa$  at different diameters (Gunthe et al., 2009; Petters et al., 2009; Rose et al., 2010; Su et al., 2010). These two methods HTDMA systems can both provide insights into the aerosol hygroscopicity at different aerosol diameters, however, they can only be used to derive aerosol hygroscopicity parameter  $\kappa$  within certain size range (usually less than 300 nm). Thus, HTDMA systems these two methods are not capable of providing more details about aerosol hygroscopicity of aerosol particles which contribute most to aerosol optical properties and aerosol liquid water contents (their diameters usually ranging from 200 nm to 1  $\mu\text{m}$ ) (Ma et al., 2012; Bian et al., 2014). The effect of aerosol water uptake on the aerosol particle light scattering ( $\sigma_{sp}$ ) (sometimes aerosol extinction coefficient (Brock et al., 2016)) is usually measured with a humidified nephelometer system. Measurements from a humidified nephelometer system can also be used to calculate the aerosol hygroscopicity parameter  $\kappa$  if the dry aerosol particle number size distribution (PNSD) is measured simultaneously (Chen et al., 2014). The enhancement factor  $f(\text{RH}, \lambda)$  which is defined as  $f(\text{RH}, \lambda) = \sigma_{sp}(\text{RH}, \lambda) / \sigma_{sp}(\text{dry}, \lambda)$ , is usually used as an indicator of how much the RH impacts on  $\sigma_{sp}$ . The scattering enhancement factor  $f(\text{RH}, \lambda)$ , defined as  $f(\text{RH}, \lambda) = \sigma_{sp}(\text{RH}, \lambda) / \sigma_{sp}(\text{dry}, \lambda)$ , characterizes changes in the aerosol scattering coefficient with RH.  $\sigma_{sp}(\text{RH}, \lambda)$  or  $\sigma_{sp}(\text{dry}, \lambda)$  represents  $\sigma_{sp}$  at wavelength  $\lambda$  at a certain RH or under dry conditions. In this research,  $f(\text{RH})$  is referred to as  $f(\text{RH}, 550 \text{ nm})$  and  $f(80\%)$  represents the  $f(\text{RH})$  at 80 % RH. The nephelometer measures aerosol optical properties of the entire aerosol size distribution, thus, the deduced  $\kappa$  value from measurements of  $f(\text{RH}, \lambda)$ . Thus,  $\kappa$  calculated from  $f(\text{RH})$  measurements represents can be understood as an overall, optically weighted  $\kappa$  and represents the overall hygroscopicity of ambient aerosol particles. This  $\kappa$  is more suitable for being used to account the influences of aerosol hygroscopic growth on aerosol optical properties compared to aerosol hygroscopicity derived from HTDMA and CCN measurements. Traditionally, derivation of  $\kappa$  from  $f(\text{RH})$  measurements requires aerosol PNSD as well as black carbon (BC) measurements to determine the imaginary part of the refractive index. As PNSD and BC measurements are expensive, their availability in field campaigns are limited. Traditionally, as mentioned before, the way of deriving  $\kappa$  values from  $f(\text{RH})$  measurements require measurements of PNSD at dry state and may also need the mass concentrations of black carbon (BC) to account the influence of BC on aerosol refractive index. However, the instruments of measuring the PNSD and BC at dry state are expensive, and during field campaigns their information is sometimes not available.

带格式的: 缩进: 首行缩进: 0 厘米

In this paper we use measurements from a field campaign on the North China Plain (NCP) to derive  $\kappa$  values using 3 methods. The first 2 methods derive  $\kappa$  from aerosol diameter hygroscopic growth and the third method derives an aerosol optical parameterization of  $\kappa$ . Method 1, labeled as  $\kappa_{f(RH)}$ , derives  $\kappa$  from aerosol PNSD, BC and nephelometer  $f(RH)$  measurements. Method 2, defined as  $\kappa_{250}$ , derives  $\kappa$  from  $g(RH)$  measurements of aerosol particles with diameter of 250 nm, using a High-Humidity Differential Mobility Analyzer (HH-TDMA). HH-TDMA is a system very similar to HTDMA but is capable of operating at higher RH points (Liu et al., 2011). Method 3, defined as  $\kappa_{sca}$ , is an empirical determination of  $\kappa$  using only nephelometer measurements of the aerosol scattering coefficient as a function of RH.

Based on detailed analysis about the relationship between  $\kappa_{f(RH)}$  and  $\kappa_{sca}$ , a novel method to directly derive  $\kappa_{f(RH)}$  based only on measurements from a humidified nephelometer system is proposed. This newly proposed approach makes it more convenient and cheaper for researchers to conduct aerosol hygroscopicity research with  $f(RH)$  measurements.

~~In this paper, with measurements from a field campaign on the North China Plain (NCP), we first derived  $\kappa$  values from measurements of  $f(RH)$  with the traditional method and then compared them with the  $\kappa$  values derived from High Humidity Tandem Differential Mobility Analyzer (HH-TDMA). HH-TDMA is a system very similar with HTDMA but is capable of operating at higher RH points (Liu et al., 2011). The relationships between  $\kappa$  values derived from  $f(RH)$  measurements and parameters used to fit measured  $f(RH)$  curves are further examined and analyzed. Finally, basing on finished analysis about the relationship between  $\kappa$  and  $f(RH)$  fitting parameters, a novel method to directly derive the aerosol hygroscopicity parameter  $\kappa$  based only on measurements from a humidified nephelometer system is proposed. This newly proposed approach makes it more convenient and cheaper for researchers to conduct aerosol hygroscopicity research with measurements of  $f(RH)$ .~~

## 2. Site description and instruments

~~In this study, the main part of used datasets is from the field campaign conducted at Wangdu (38°40'N, 115°08'E) during summer on the North China Plain (NCP). This field campaign was jointly conducted by Peking University, China and Leibniz Institute for Tropospheric Research, Germany. Wangdu site is located in the suburban district of Wangdu County, Hebei Province, China and situated adjacent to farmland and residential areas, it belongs to the typical region of the NCP. This observation~~

带格式的：首行缩进：2 字符

campaign lasted for about one month from 4 June, 2014 to 14 July, 2014. The measured  $f(RH, \lambda)$  dataset was available from June 21<sup>st</sup>, 2014, to July 1<sup>st</sup>, 2014.

For datasets from Wangdu campaign. The chemical compositions of the aerosol particles with an aerodynamic diameter of less than 2.5  $\mu\text{m}$  (PM<sub>2.5</sub>) were analyzed based on the samples collected on quartz and Teflon filters. Other instruments share one inlet which is placed on the roof of the container. Regarding this inlet system, aerosol particles first entered an impactor which selected the aerosol particles with an aerodynamic diameter of less than 10  $\mu\text{m}$ , and then passed through a dryer which is capable of reducing the RH of the sample air to lower than 30 %. In succession, the sample air passed through a splitter and was allotted to different instruments according to their required flow rates. The PNSD at dry state ranging from 3nm to 10 $\mu\text{m}$  was observed jointly by a Twin Differential Mobility Particle Sizer (TDMPS, Leibniz Institute for Tropospheric Research (IFT), Germany; Birmili et al. (1999)) and an Aerodynamic Particle Sizer (APS, TSI Inc., Model 3321) with a temporal resolution of 10 minutes. The absorption coefficient at 637 nm was measured using a Multi-angle Absorption Photometer (MAAP Model 5012, Thermo, Inc., Waltham, MA USA) with a temporal resolution of 1 minute, and further used to calculate the mass concentrations of black carbon (BC) with a constant mass absorption efficiency (MAE) of 6.6  $\text{m}^2\text{g}^{-1}$ . The growth factors of aerosol particles at six selected particle diameters (30 nm, 50 nm, 100 nm, 150nm, 200 nm and 250 nm) at 98% RH condition were obtained from the measurements of the HH-TDMA (Leibniz Institute for Tropospheric Research (IFT), Germany; Hennig et al. (2005)). The  $f(RH, \lambda)$  curves of aerosol particles with RH ranging from about 50% to 90% were measured by a humidified nephelometer system which consists of two three-wavelength integrating nephelometers (TSI Inc., Model 3563) and a humidifier. The humidifier was used to moisten the air which will be sampled into the second nephelometer. Details of this humidified nephelometer system please refer to (Kuang et al., 2016a).

PNSDs at dry state and mass concentrations of BC derived from MAAP measurements measured at both Wuqing from 12 July to 14 August in 2009 and Xianghe from 9 July to 8 August in 2013 are also used in this study to examine the influence of PNSD and BC on derivation of  $\kappa$  values from  $f(RH)$  measurements and other relationships. Additionally,  $\sigma_{\text{sp}}$  values which were observed during these three field campaigns introduced before with a three-wavelength integrating nephelometer (TSI Inc., Model 3563) are also used in Sect.4.3. Both Wuqing and Xianghe are representative regional background sites of the NCP and locates in the northern part of the NCP. Details about these two

campaigns can be found in papers published by Kuang et al. (2015) and Ma et al. (2016).

Datasets from five field campaigns are used in this paper. The five campaigns are conducted at four different measurements sites of the North China Plain (NCP) (Wangdu, Xianghe and Gucheng in Hebei province and Wuqing in Tianjin, and site locations are shown in Fig.S1). Time periods and used datasets from these field campaigns are listed in Table 1.

During these field campaigns, sampled aerosol particles have aerodynamic diameters less than 10  $\mu\text{m}$  (selected by passing through an impactor). Aerosol PNSDs with particle diameter ranging from 3nm to 10 $\mu\text{m}$  were jointly measured by a Twin Differential Mobility Particle Sizer (TDMPS, Leibniz-Institute for Tropospheric Research (IfT), Germany; Birmili et al. (1999)) or a scanning mobility particle size spectrometer (SMPS) and an Aerodynamic Particle Sizer (APS, TSI Inc., Model 3321) with a temporal resolution of 10 minutes. The mass concentrations of BC were measured using a Multi-angle Absorption Photometer (MAAP Model 5012, Thermo, Inc., Waltham, MA USA) or an aethalometer called AE33 (Drinovec et al., 2015). The aerosol light scattering coefficients ( $\sigma_{sp}$ ) at three wavelengths were measured using a TSI 3563 nephelometer (Anderson and Ogren, 1998) or an Aurora 3000 nephelometer (Müller et al., 2011).

A humidified nephelometer system consists of two nephelometers and a humidifier was used in Wangdu and Gucheng campaigns. For the humidified nephelometer systems that we have designed, they only scan the hydration branch of the aerosol hygroscopic growth. The humidifier humidified the sample air through a Gore-Tex tube. The water vapor penetrates through the Gore-Tex tube, which is surrounded by a circulating water layer in a stainless steel tube. The temperature cycle of the circulating water layer was specified and controlled by a water bath. During Wangdu campaign, only one water bath was used, for each RH scanning cycle, the temperature cycle was fixed. Thus, the RH range of each cycle will change. Since the room temperature of the container was relatively stable during Wangdu campaign, the RH points of  $f(\text{RH})$  cycles range from about 50% to about 90%, and each cycle lasted about 45 minutes. However, one cycle cost about 90 minutes because after each cycle was finished, the water bath needed about another 45 minutes to cool. During Gucheng campaign, this problem is solved by using two water baths and they provided circulating water alternatively for the humidifier. The corresponding temporal resolution of  $f(\text{RH})$  cycles was about 45 minutes. In addition, a control software system was developed and can make sure the RH scans within certain RH range. During Gucheng campaign, the RH points of each  $f(\text{RH})$  cycle range from 45% to 90%.

During Wangdu campaign, the two nephelometers operated in series, used nephelometer was TSI 3563. During Gucheng campaign, the two nephelometers operated in parallel, used nephelometer was Aurora 3000. In the following, we refer the nephelometer which measures  $\sigma_{sp}$  in dry state and the nephelometer which measures  $\sigma_{sp}$  at different RH points as dry Neph and wet Neph, respectively. Two combined RH and temperature sensors (Vaisala HMP110; accuracy of  $\pm 0.2$  °C and  $\pm 1.7$  % for RH ranges from 0 to 90 %, respectively, and accuracy of  $\pm 2.5$  % for RH ranges from 90 % to 100 % according to the manufacturer) are placed at the inlet and outlet of the wet Neph, and the measured RHs and temperatures are defined as  $RH_1/T_1$  and  $RH_2/T_2$ , respectively. The dew points at the inlet and outlet of wet Neph were calculated using the measured  $RH_1/T_1$  and  $RH_2/T_2$ , and the average value was considered as the dew point of the sample air. The sample RH can be calculated through the derived dew point and the sample temperature which is measured by the sensor inside the sample cavity of the nephelometer. During Wangdu campaign, measurements from the humidified nephelometer system were only available from 21 June, 2014, to 1 July, 2014. During the two campaigns, the two nephelometers were calibrated every two weeks. The manufacturer of HMP110 suggests that the sensors should be calibrated yearly. We didn't calibrate the used HMP110 sensors during the two campaigns because they only have been used less than three months, and results of cross checks showed that they agree well with each other. The sample RHs in the dry Neph were about 20% and about 8% during Wangdu and Gucheng campaigns, respectively.

Dataset includes aerosol PNSDs at dry state, mass concentrations of BC and  $\sigma_{sp}$  values of different wavelengths from the following four campaigns which are listed in Table 1 are referred to as dataset D1: two campaigns conducted in Wuqing, Xianghe campaign, Wangdu campaign before 21 June, 2014. Note that  $\sigma_{sp}$  values of dataset D1 are not corrected. However, for  $\sigma_{sp}$  values shown in Fig.1, the truncation errors are corrected using Mie theory with measured PNSD and mass concentrations of BC.

During Wangdu campaign, the growth factors of aerosol particles at six selected particle diameters (30 nm, 50 nm, 100 nm, 150nm, 200 nm and 250 nm) at 98% RH condition were obtained from the measurements of the HH-TDMA (Leibniz-Institute for Tropospheric Research (IfT), Germany; Hennig et al. (2005)). Detailed information about HH-TDMA measurements please refer to Liu et al. (2011)

### 3. Methodology

#### 3.1 Calculations of hygroscopicity parameter $\kappa$ from $f(RH)$ measurements ~~of $f(RH)$~~ and

## HH-TDMA

Research of Chen et al. (2014) demonstrated that if the PNSD at dry state is measured, then measurements of  $f(\text{RH})$  can be used to derive the aerosol hygroscopicity parameter  $\kappa$  by conducting an iterative calculation with the Mie theory and the  $\kappa$ -Köhler theory. To reduce the influence of random errors of observed  $f(\text{RH})$  at a certain RH, all valid  $f(\text{RH})$  measurements in a complete humidifying cycle is used in the derivation algorithm. The retrieved  $\kappa$  is the  $\kappa$  value which can be used to best fit the observed  $f(\text{RH})$  curve, labelled as  $\kappa_{f(\text{RH})}$ , and this method of deriving  $\kappa$  is Method 1. Details about this retrieval algorithm is described in Chen et al. (2014). Of particular note is that in this research the mass concentration of BC is also considered in the retrieval algorithm to account for the influence of BC on refractive indices of aerosol particles at different sizes. During the simulating process, aerosol components are divided into two classes in terms of their optical properties: the light absorbing component (i.e. BC) and less absorbing components (comprising inorganic salts and acids such as sulfates, nitrates, ammoniums, as well as most of the organic compounds). The BC is considered to be homogeneously mixed with other aerosol components, and the mass size distribution of BC used in Ma et al. (2012) which is observed on the NCP is used in this research to account the mass distributions of BC at different particle sizes. The used refractive index and density of BC are  $1.80 - 0.54i$  and  $1.5\text{g cm}^{-3}$  (Kuang et al., 2015). Used refractive indices of non light-absorbing aerosol components (other than BC) and liquid water are  $1.53 - 10^{-7}i$  (Wex et al., 2002) and  $1.33 - 10^{-7}i$  (Seinfeld and Pandis, 2006), respectively. The flow chart about this retrieval algorithm is also introduced in the supporting information, please refer to Fig.S2 for more details.

The HH-TDMA measures hygroscopic growth factors of particles at different sizes at 98% RH condition. The measured hygroscopic factors can be directly related to  $\kappa$  with equation (1). For a specified size of selected aerosol particles, a distribution of growth factors can be measured, and thus can be used to derive a probability distribution of  $\kappa$  and finally come to the calculation of average  $\kappa$  value corresponding to this size of aerosol particles. The method on how to derive average  $\kappa$  value of certain size of aerosol particles from HH-TDMA measurements is elaborately described in Liu et al. (2011). In this research  $\kappa$  values derived from  $g(\text{RH})$  measurements of aerosol particles with diameter of 250 nm are used, defined as  $\kappa_{250}$ . This method of deriving  $\kappa$  is Method 2.

### 3.2 Parameterization schemes for $f(\text{RH})$

域代码已更改



Due to the complex chemical compositions of ambient aerosol particles and the challenge in precisely measuring their molecular compositions, it is difficult to directly describe the influence of RH on  $\sigma_{sp}$ . Some simplified parameterization schemes are usually used to describe  $f(RH)$  as a function of RH. The most frequently used  $f(RH)$  parameterization scheme is a power-law function which is known as “gamma” parameterization (Quinn et al., 2005; Hänel, 1981) (Hänel, 1981) and the formula of this single-parameter representation is written as the following:

$$f(RH) = \left[ \frac{(100 - RH_0)}{100 - RH} \right]^\gamma \quad (2)$$

where  $RH_0$  is the RH of dry condition, and  $\gamma$  is a parameter fitted to the observed  $f(RH)$ . In this study, we estimated  $\gamma$  values with observed  $f(RH)$  curves and for the first time to our knowledge, we further examined the relationship between  $\gamma$  and  $\kappa_{f(RH)}$ — $\kappa$  retrieved from  $f(RH)$  measurements.

Recently, a new physically based single-parameter representation was proposed by Brock et al. (2016) to describe  $f(RH)$ . Their results demonstrated that this proposed parameterization scheme can better describe  $f(RH)$  than the widely used gamma power-law approximation (Brock et al., 2016). The formula of this new scheme is written as:

$$f(RH) = 1 + \kappa_{sca} \frac{RH}{100 - RH} \quad (3)$$

where  $\kappa_{sca}$  is a parameter fitted to observed  $f(RH)$  best. Here, we give a brief introduction about the physical understanding of this alternative parameterization scheme. Regardless of the curvature effects for particle diameters larger than 100 nm, the hygroscopic growth factor for aerosol particles can be approximately expressed as the following (Brock et al., 2016):  $gf_{diam} \cong (1 + \kappa \frac{RH}{100 - RH})^{1/3}$ . Moreover,  $\sigma_{sp}$  is usually approximately proportional to total aerosol volume (Pinnick et al., 1980) which means that the relative change in  $\sigma_{sp}$  due to aerosol water uptake is roughly proportional to relative change in aerosol volume. The enhancement factor in volume can be expressed as the cube of  $gf_{diam}$ , thus lead to the formula form of  $f(RH)$  expressed in equation (3). More details about the discussion of this new expression form of  $f(RH)$  can be found in the paper published by Brock et al. (2016). In this paper, the performance of this newly proposed scheme is investigated, values of  $\kappa_{sca}$  are estimated from observed  $f(RH)$  curves and their relationship with  $\kappa$  values retrieved from  $f(RH)$  measurements is also examined.

During processes of measuring  $f(\text{RH})$ , the sample RH in the dry Neph ( $\text{RH}_0$ ) is not zero. According to equation (3), the measured  $f(\text{RH})_{\text{measure}} = \frac{f(\text{RH})}{f(\text{RH}_0)}$  should be fitted using the following formula:

$$f(\text{RH})_{\text{measure}} = (1 + \kappa_{\text{sca}} \frac{\text{RH}}{100 - \text{RH}}) / (1 + \kappa_{\text{sca}} \frac{\text{RH}_0}{100 - \text{RH}_0}) \quad (4)$$

The method of calculating  $\kappa_{\text{sca}}$  by curve fitting using equation (4) is called Method 3. These two parameterization schemes which are introduced here are referred to as  $\gamma$ -Method and  $\kappa_{\text{sca}}$ -Method respectively in the following paragraphs.

#### 4. Results and discussions

##### 4.1 Derived $\kappa$ values from $f(\text{RH})$ and HH-TDMA measurements

During this field campaign, the aerosol physical, chemical and optical properties are synergistically observed with different types of instruments. They provide valuable datasets to perform an insightful analysis about aerosol hygroscopicity and its relationship with other aerosol properties. The time series of  $\sigma_{\text{sp}}$  at 550 nm at dry state are shown in Fig.1a, and values of  $\sigma_{\text{sp}}$  at 550 nm shown in Fig.1a are corrected from measurements of TSI 3563 nephelometer. The results show that this observation period has experienced varying degrees of pollution levels, with  $\sigma_{\text{sp}}$  at 550 nm ranging from 15 to 1150  $\text{Mm}^{-1}$ . The aerosol chemical compositions also change a lot during the observation period (Kuang et al., 2016a). The relative contributions of mass concentrations of organic matter to total PM<sub>2.5</sub> mass concentrations range from 2% to 42%. Moreover, the relative contributions of mass concentrations of sulfate, nitrate and ammonium to total PM<sub>2.5</sub> mass concentrations range from 5 to 50 %, 2 to 27 % and 1 to 21 %, respectively (Kuang et al., 2016a). These results imply that during this observation period, the aerosol hygroscopicity changes a lot whereafter corroborated by  $f(\text{RH})$  measurements. Overall,  $f(80\%)$  values range between 1.1 and 2.3 with an average of 1.8. Periods when deliquescent phenomena occur,  $f(80\%)$  values are relatively higher with a variation range of 1.7 to 2.3 and their average is 2.0. This is because of the dominance of ammonium sulfate during periods when deliquescent phenomena occur. More detailed analysis about the frequently observed deliquescent phenomena during this field campaign please refer to (Kuang et al., 2016a). Furthermore,  $\kappa$  values derived from  $f(\text{RH})$  measurements by combining measurements of PNSD at dry state and mass concentrations of BC. Values of  $\kappa_{f(\text{RH})}$  derived from Method 1 are shown in Fig.1b. During deliquescent phenomena periods,  $f(\text{RH})$  jumps when sample RH in the cavity of the

带格式的：缩进：首行缩进： 0.85 厘米

带格式的：缩进：首行缩进： 6.5 字符

带格式的：缩进：首行缩进： 0 字符

nephelometer mainly ranges from 60 % to 65 %. Therefore, for a humidifying cycle which shows jump phenomenon in  $f(\text{RH})$ , only  $f(\text{RH})$  points when RHs are greater than 70% (after the jump point) are used to retrieve  $\kappa$ . During deliquescence  $f(\text{RH})$  exhibits an abrupt increase between RH values of 60-65%. As such, only  $f(\text{RH})$  data points with  $\text{RH} > 70\%$  were used in determination of  $\kappa_{f(\text{RH})}$  when deliquescence was apparent. For  $f(\text{RH})$  cycles without deliquescence, all  $f(\text{RH})$  points are used in the retrieval algorithm with RH ranges of about 50% to 90%. The results demonstrate that  $\kappa$  derived from  $f(\text{RH})$  measurements (hereinafter referred to as  $\kappa_{f(\text{RH})}$ ) lies between 0.06 and 0.5143, with an average of 0.32. The lowest  $\kappa_{f(\text{RH})}$  values are found when the air quality is relatively clean ( $\sigma_{sp}$  at 550 nm is lower than  $100 \text{ Mm}^{-1}$ ) on 27 and 28 June. During these two days, organic matter dominates the mass concentration of PM<sub>2.5</sub> which results in the low hygroscopicity of aerosol particles (Kuang et al., 2016a). On the contrary, the largest  $\kappa_{f(\text{RH})}$  values are found during periods when deliquescent phenomena occur and inorganic chemical compositions dominate the mass concentrations of PM<sub>2.5</sub>, especially, sulfate is highly abundant during these periods. Of particular note is that during relatively polluted periods ( $\sigma_{sp}$  at 550 nm larger than  $100 \text{ Mm}^{-1}$ ) aerosol particles are generally very hygroscopic which imply that aerosol water uptake can exert significant impacts on regional direct aerosol radiative effect and ambient visibility during this observation period. On the whole, the average  $\kappa_{f(\text{RH})}$  during this observation period is 0.28.

On the basis of the average size-resolved  $\kappa$  distribution from Haze in China (HaChi) campaign (Liu et al., 2014),  $\kappa$  values change a lot for aerosol particles whose diameters are less than 250 nm, however,  $\kappa$  values vary relatively smaller for aerosol particles whose diameter range from 250 nm to 1  $\mu\text{m}$ . In addition, the results from HaChi campaign also demonstrate that aerosol particles whose diameter range from 200 nm to 1  $\mu\text{m}$  usually contribute more than 80% to  $\sigma_{sp}$  at 550 nm during summer on the NCP (Ma et al., 2012). That is,  $\kappa_{f(\text{RH})}$  may share similar magnitude with  $\kappa_{250}$ . To compare  $\kappa$  values derived from Method 1 and Method 2 measurements of humidified nephelometer system and HH TDMA, average  $\kappa$  values corresponding to aerosol particles at only 250 nm which are derived from HH TDMA measurements values of  $\kappa_{250}$  are also shown in Fig. 1b. In the following, average  $\kappa$  which is derived from HH TDMA measurements for aerosol particles having particle size of 250 nm is referred to as  $\kappa_{250}$ . During this observation period, values of  $\kappa_{250}$  range from 0.11 to 0.56, with an average of 0.34 which is very close to average  $\kappa_{250}$  observed during HaChi campaign

(Liu et al., 2011). The results shown in Fig.1b suggest that, in general,  $\kappa_{f(RH)}$  values agree well with  $\kappa_{250}$  values, however, are usually lower than  $\kappa_{250}$  values. To quantitatively compare these two types of  $\kappa$  values, they are plotted against each other and shown in Fig.2. It can be seen that they are highly correlated but overall, the  $\kappa_{250}$  values are systematically higher than  $\kappa_{f(RH)}$  values, and the average difference between  $\kappa_{250}$  and  $\kappa_{f(RH)}$  is 0.026. The statistical relationship between  $\kappa_{250}$  and  $\kappa_{f(RH)}$  is also shown in Fig.2. This relationship may be useful for researchers if they want to estimate the influences of aerosol water uptake on aerosol optical properties and aerosol liquid water contents when only HH-TDMA or HTDMA measurements are available.

A model experiment is conducted to better understand the relationship between  $\kappa_{250}$  and  $\kappa_{f(RH)}$ . During HaChi campaign, size-resolved  $\kappa$  distributions are derived from measured size-segregated chemical compositions (Liu et al., 2014) and their average is used in this experiment to account the size dependence of aerosol hygroscopicity which is shown in Fig. 3a. With this fixed average size-resolved  $\kappa$  distribution, all observed PNSDs at dry state along with mass concentrations of BC which are observed at three different representative background sites of the NCP during summer from dataset D1 are used to simulate the retrieval of  $\kappa_{f(RH)}$  under different PNSD and BC conditions. Field campaigns conducted at these three sites are introduced in Sect.2. The treatment of BC is the same with the way in the process of deriving  $\kappa_{f(RH)}$  which is introduced in Sect.4.1. The used PNSDs shown in Fig.3b show indicate that large varying types of PNSDs are considered in the simulative experiment. As to the simulating process, with given PNSD, mass concentration of BC and size-resolved  $\kappa$  distribution. The first step is simulating  $f(RH)$  points using Mie theory and  $\kappa$ -Köhler theory with RH range of 50% to 90% and the RH interval is 10%. The second step is retrieving corresponding  $\kappa_{f(RH)}$  using the procedure of Method 1. The  $\kappa$  value at particle diameter of 250 nm of the used size-resolved  $\kappa$  distribution is the corresponding  $\kappa_{250}$ . The probability distribution of simulated  $\kappa_{f(RH)}$  is also shown in Fig.3a. The standard deviation of retrieved  $\kappa_{f(RH)}$  is about 0.01 which suggests that if the size-resolved  $\kappa$  distribution is fixed, then  $\kappa_{f(RH)}$  varies little. Due to  $\kappa_{f(RH)}$  represents an overall, optically-weighted size-integrated  $\kappa$ , it is clearly shown in Fig.3a that in most cases  $\kappa_{f(RH)}$  values are located between  $\kappa$  values of aerosol particles ranging from 200 nm to 1  $\mu$ m. Moreover, about 70% of simulated  $\kappa_{f(RH)}$  values are less than  $\kappa_{250}$  which to some extent explains the observed difference between  $\kappa_{250}$  and  $\kappa_{f(RH)}$  mentioned before. However, the simulated average difference

between  $\kappa_{250}$  and average  $\kappa_{f(RH)}$  is about 0.01 which is ~~far~~ less than the observed averaged difference between  $\kappa_{250}$  and  $\kappa_{f(RH)}$  which is 0.026. Especially, when  $\kappa_{f(RH)}$  values are relatively lower ( $< 0.25$ ), the  $\kappa_{250}$  is systematically higher than  $\kappa_{f(RH)}$ . Except that uncertainties from measurements of instruments, for example, the uncertainty of RH in measurements of HH-TDMA and uncertainties of measuring  $f(RH)$  (details about the uncertainty sources of  $f(RH)$  measurements can be found in the paper published by Titos et al. (2016)), there are other two reasons may be associated with this discrepancy between  $\kappa_{250}$  and  $\kappa_{f(RH)}$ . The first one is that configurations of size-resolved  $\kappa$  distributions and PNSDs during this field campaign are far different from the model experiment. The second one is that in the real atmosphere,  $\kappa$  values at different RH conditions may be different (You et al., 2014) and most of  $f(RH)$  measurements are conducted when RH is lower than 90%, however, the measurements of HH-TDMA are conducted when RH is equal to 98%. Overall, the observed general consistency between  $\kappa$  values derived from measurements of  $f(RH)$  and HH-TDMA confirms the reliability of  $\kappa$  values derived from  $f(RH)$  measurements.

#### 4.2 Relationships between $\kappa$ derived from $f(RH)$ measurements and $f(RH)$ fitting parameters

In the previous section, ~~the overall properties of ambient aerosol particles are introduced,~~ derived  $\kappa_{f(RH)}$  values are characterized and compared with  $\kappa_{250}$  values. These results demonstrated that derived  $\kappa_{f(RH)}$  values can commendably represent variations of aerosol hygroscopicity of ambient aerosol populations. In this section, the relationship between derived  $\kappa_{f(RH)}$  values and  $f(RH)$  fitting parameters are further examined to investigate their relationships.

Two parameterization schemes of  $f(RH)$  are discussed in this paper, including the ~~currently widely used  $\gamma$ -Method and the newly proposed  $\kappa_{sea}$ -Method by Brock et al. (2016). and both methods are introduced in Sect.3.2. A fitting example of these two methods is shown in Fig.4A. For  $f(RH)$  cycles observed during this field campaign, they are fitted by using both  $\gamma$  Method and  $\kappa_{sea}$  Method, corresponding values of  $\gamma$  and  $\kappa_{sea}$  are also deduced. Values of  $\gamma$  and  $\kappa_{sea}$  are fitted from observed  $f(RH)$  cycles. For cycles during deliquescent periods, only  $f(RH)$  points with RH higher than 70% are used to perform fitting processes. The fitting performance of these two methods are further investigated by conducting the comparison between measured and fitted  $f(85)\%$  values. Probability distributions of the ratio between fitted and measured  $f(85)\%$  by using these two methods are shown in Fig.4B. The results indicate that in most cases both  $\gamma$  Method and  $\kappa_{sea}$  Method~~

fit observed  $f(\text{RH})$  cycles well with  $\gamma$  Method performs slightly better which is contrary to the results introduced by Brock et al. (2016), their results demonstrate that  $\kappa_{\text{sca}}$  Method can better describe observed  $f(\text{RH})$  than  $\gamma$  Method. That is to say,  $f(\text{RH})$  curves observed at different places or time periods may require different parameterization schemes to fit them best, however, in general both  $\gamma$  Method and  $\kappa_{\text{sca}}$  Method are good approaches to fit observed  $f(\text{RH})$  curves.

Concerning  $\gamma$  Method, previous studies usually examine the relationship between  $\gamma$  and aerosol chemical compositions and established several parameterization schemes to fit  $\gamma$  with mass fractions of different aerosol chemical compositions, including organic materials, sulfate and nitrate (Quinn et al., 2005; Titos et al., 2014; Zhang et al., 2015). However, to obtain a reliable estimation of  $\gamma$ , complete information of aerosol chemical compositions may be required which is difficult to get, and it is also hard to find a comprehensive description of  $\gamma$  based on those complicated chemical compositions. Single aerosol hygroscopicity parameter  $\kappa$  can represent overall hygroscopicity of aerosol particles which contains influences of different chemical compositions on aerosol hygroscopicity, therefore may be used to better fit  $\gamma$ . In view of this, the relationship between  $\kappa_{f(\text{RH})}$  and  $\gamma$  is investigated and shown in Fig. 4aC. It is found that a pretty good an approximately linear relationship exists (square of correlation coefficient is 0.905) between  $\kappa_{f(\text{RH})}$  and  $\gamma$ , especially when  $\kappa_{f(\text{RH})}$  is larger than 0.245. This correlation is far better than previously found relationships between  $\gamma$  and aerosol chemical compositions (Quinn et al., 2005; Titos et al., 2014; Zhang et al., 2015) and statistical parameters which can be used to parameterize  $\gamma$  with  $\kappa_{f(\text{RH})}$  is also shown in Fig. 4C. During this field campaign, fitted  $\gamma$  ranges from 0.135 to 0.5663 with an average of 0.416.

Furthermore, during this field campaign, fitted  $\kappa_{\text{sca}}$  ranges from 0.05 to 0.36 with an average of 0.22. The relationship between  $\kappa_{f(\text{RH})}$  and  $\kappa_{\text{sca}}$  is also investigated and shown in Fig. 4b. and It is found a strong linear relationship also exists (square of correlation coefficient is 0.978) between  $\kappa_{f(\text{RH})}$  and  $\kappa_{\text{sca}}$ . This linear relationship is even better than the linear relationship between  $\kappa_{f(\text{RH})}$  and  $\gamma$ . Not only that, the statistically fitted line almost passes through zero point which implies that a proportional relationship may exist between  $\kappa_{f(\text{RH})}$  and  $\kappa_{\text{sca}}$ . This strong correlation should be intrinsic due to the idea of  $\kappa_{\text{sca}}$ -Method is from the linkage between total aerosol volume and  $\sigma_{\text{sp}}$  as introduced in Sect. 3.2 and the increase of total aerosol volume due to aerosol water uptake is directly linked to the overall aerosol hygroscopicity parameter  $\kappa$ . It seems that this promising linear relationship can help bridge the gap between  $f(\text{RH})$  and  $\kappa$ . However, results from Brock et al. (2016)

imply demonstrated that the relationship between  $\kappa_{f(RH)}$  and  $\kappa_{sca}$  is much more sophisticated and it is affected by both aerosol hygroscopicity and PNSD at dry state. In the paper published by Brock et al. (2016),  $\kappa_{ext}$  (a parameter determined from measurements of the aerosol extinction coefficient as a function of RH using formula form of equation (2)) and  $\kappa_{chem}$  (a constant  $\kappa$  determined from chemical constituents of entire aerosol population) are used and correspond to  $\kappa_{sca}$  and  $\kappa_{f(RH)}$  in this research, the difference between  $\kappa_{ext}$  and  $\kappa_{sca}$  is that  $\kappa_{ext}$  is used to fit the light enhancement factor of aerosol extinction coefficient,  $\kappa_{chem}$  and  $\kappa_{f(RH)}$  actually means the same because both them are overall and size independent hygroscopicity parameters. Results from Brock et al. (2016) concluded that the ratio  $\kappa_{ext}/\kappa_{chem}$  generally lies between 0.6 to 1 which implies that the ratio  $\kappa_{sca}/\kappa_{f(RH)}$  (in the following, this ratio is referred to as  $R_k$ ) also should have large variations and may share a similar range of variability shares the similar variation range. By revisiting the relationship between  $\kappa_{f(RH)}$  and  $\kappa_{sca}$  found in this research, it can be found that  $R_k$  during this field campaign ranges from 0.586 to 0.77 with an average of 0.697. This result suggests that if we directly establish a linkage between  $\kappa_{f(RH)}$  and  $\kappa_{sca}$  with an average  $R_k$  can result in a non-negligible bias (relative difference can reach about 15%). Besides, this range of  $R_k$  only represents the relationship between  $\kappa_{f(RH)}$  and  $\kappa_{sca}$  during a short time period and at only one site.

To better understand the relationship between  $\kappa_{f(RH)}$  and  $\kappa_{sca}$ , all PNSDs at dry state (shown in Fig.3a) along with mass concentrations of BC observed from three different representative background sites of the NCP during summer which is introduced in Sect.2 from dataset D1 are used to simulate the relationship between  $\kappa_{f(RH)}$  and  $\kappa_{sca}$  with Mie and  $\kappa$ -Köhler theories. The aim of including PNSD and BC information from different campaigns is to simulate variations of  $R_k$  under different conditions. During simulating processes, for each PNSD, we change  $\kappa_{f(RH)}$  from 0.01 to 0.76 with an interval of 0.01 to examine the influence of aerosol hygroscopicity on  $R_k$ . The way of treating BC is same with the simulation experiment introduced in Sect.4.1. For each PNSD and  $\kappa_{f(RH)}$ , the simulating processes include two steps. The first step is simulating  $f(RH)$  points using Mie theory and  $\kappa$ -Köhler theory with RH range of 50% to 90% and the RH interval is 10%. The way of treating BC is same with the retrieval procedure of  $\kappa_{f(RH)}$  introduced in Sect.3.1. The second step is retrieving the corresponding  $\kappa_{f(RH)}$  using the procedure of Method 1 and calculating  $\kappa_{sca}$  with Method 3. Simulated results of  $R_k$  are shown in Fig.5a and the probability distribution of simulated  $R_k$  values is shown in Fig.5b. The results show that  $R_k$  primarily ranges from 0.55 to 0.842 with an average of

0.69 which is ~~same with~~ ~~very close to~~ the average  $R_K$  measured during Wangdu campaign ~~the field~~  
~~campaign of this research~~. These results also indicate that the relationship between  $\kappa_{f(RH)}$  and  $\kappa_{sca}$   
is much more complex than a simple linear relationship and more information about aerosol properties  
are necessary to gain insights into the variation of  $R_K$ .

#### 4.3 A novel method to directly derive $\kappa$ from measurements of a humidified nephelometer system

A robust linear relationship is ~~first~~ found between  $\kappa_{f(RH)}$  and  $\kappa_{sca}$  in Sect.4.2 ~~and then it turns~~  
~~out that the relationship between  $\kappa_{f(RH)}$  and  $\kappa_{sca}$  is much more complex than that shown in Fig.4D,~~  
however, results of further analysis suggest that  $R_K$  varies a lot. The complexity comes from ~~large~~  
~~variations of  $R_K$  and that~~ both PNSD at dry state and aerosol hygroscopicity have impacts on  $R_K$ .  
Generally, used nephelometer of a humidified nephelometer system have three wavelengths (Titos et  
al., 2016) and the spectral dependence of  $\sigma_{sp}$  is usually described by the following Ångström  
formula:  $\sigma_{sp}(\lambda) = \beta \lambda^{-\alpha_{sp}}$ , where  $\beta$  is the particle number concentration dependent coefficient,  $\lambda$  is  
the wavelength of light and  $\alpha_{sp}$  represents the Ångström exponent of  $\sigma_{sp}$  ~~(Zieger et al., 2014)~~.  
~~Thus,~~ Ångström exponent can be directly inferred from the measurements of  $\sigma_{sp}$  at different  
wavelengths. Of particular note is that Ångström exponent ~~can~~ not only ~~can~~ be used to account the  
spectral course of  $\sigma_{sp}$ , it also reveals information about PNSD. In general, larger value of Ångström  
exponent corresponds to smaller aerosol particles. That is, Ångström exponent can be a proxy of  
PNSD at dry state and be used in the processes of estimating the impacts of PNSD on  $R_K$ . On the other  
hand, with regard to aerosol hygroscopicity, although  $R_K$  varies within certain range, value of  $\kappa_{sca}$   
can still be used to represent the overall hygroscopicity of aerosol particles. Given this, simulated  $R_K$   
values introduced in the last paragraph of Sect.4.2 are spread into a two dimensional gridded plot. The  
first dimension is Ångström exponent with an interval of 0.02 and the second dimension is  $\kappa_{sca}$   
with an interval of 0.01, average  $R_K$  value within each grid is represented by color and shown in  
Fig.6a. Values of Ångström exponent corresponding different PNSDs are calculated from  
concurrently measured  $\sigma_{sp}$  values at 450 nm and 550 nm from TSI 3563 nephelometer. Based ~~ing~~ on  
results shown on Fig.6a, the different impacts of aerosol hygroscopicity and ~~PNSD at dry state dry~~  
~~scattering~~ Ångström exponent on  $R_K$  can be ~~clearly~~ distinguished to some extent. The results



500 demonstrate that PNSD at dry state ~~dominates~~ play a more important role in the variations of  $R_k$  than  
501 overall aerosol hygroscopicity, ~~nevertheless, aerosol hygroscopicity has non negligible impacts.~~  
502 Overall, larger value of Ångström exponent corresponds to higher  $R_k$ . ~~However, a~~ Aerosol  
503 hygroscopicity exhibits different influences on  $R_k$  when Ångström exponent values are different.  
504 On average ~~Generally speaking~~, higher  $\kappa_{sca}$  corresponds to lower  $R_k$  if Ångström exponent is  
505 smaller than about 0.8 and higher  $\kappa_{sca}$  corresponds to higher  $R_k$  if Ångström exponent is larger  
506 than about 1.6.–

507 ~~In addition,~~ The percentile value of standard deviation of  $R_k$  values within each grid of Fig.6a  
508 divided by their average is shown in Fig.6b. The Ångström exponent only represents an overall size  
509 property of aerosol particles, the same Ångström exponent corresponds to different aerosol PNSDs.  
510 Within each grid of Fig.6a, the same  $\kappa_{sca}$  corresponds to different combinations of aerosol PNSD  
511 and  $\kappa_{f(RH)}$ , and  $R_k$  values also change. Note that the size-dependent chemical composition also  
512 exerts influence on  $R_k$ . However, if PNSD is fixed, each size-resolved  $\kappa$  distribution corresponds to  
513 a certain  $\kappa_{f(RH)}$ , and  $\kappa_{f(RH)}$  varies with certain range no matter how size-resolved  $\kappa$  distribution  
514 changes. Therefore, influences of size-dependent chemical compositions on  $R_k$  are already included  
515 in the simulated results of producing the look up table by varying the  $\kappa_{f(RH)}$  from 0 to 0.7 for a fixed  
516 aerosol PNSD.

517 As shown in Fig.6b, ~~In~~ in most cases, these percentile values are less than 6% (about ~~89~~0%) which  
518 demonstrates that  $R_k$  varies little within each grid shown in Fig.6a. This implies that results of Fig.6a  
519 can be used as a look up table to estimate  $R_k$ . As what's introduced before, currently ~~widely~~-used  
520 nephelometer of a humidified nephelometer system usually have three wavelengths (Titos et al., 2016),  
521 thus can provide information about Ångström exponent, and  $\kappa_{sca}$  can be directly fitted from  
522 observed  $f(RH)$  curve. Even only one  $f(RH)$  point is measured,  $\kappa_{sca}$  can still be calculated from  
523 equation (43). ~~Therefore,~~ Using results shown in Fig.6a as a look up table,  $R_k$  values can be directly  
524 predicted from measurements of a humidified nephelometer system. With this method,  $R_k$  values  
525 during this Wangdu field campaign are predicted (values of Ångström exponent are calculated from  
526 measured  $\sigma_{sp}$  values at 450 nm and 550 nm under dry conditions) and compared with measured  $R_k$   
527 values, the results are shown in Fig.7a. The Ångström exponent during this field campaign ranges  
528 from 0.63 to 1.96 with an average of 1.4. It can be seen from Fig.7a that majority of points lie nearby

1:1 line and 82.92% points have relative differences less than 6% which is consistent with results shown in Fig.6b. This result is quite promising and can be further used to derive  $\kappa_{f(RH)}$  values by combining fitted  $\kappa_{sca}$  and predicted  $R_k$ . This method of deriving  $\kappa_{f(RH)}$  is called Method 4 and include two steps. The first step is calculating Ångström exponent based on measured  $\sigma_{sp}$  values at 450 nm and 550 nm by the dry nephelometer and calculating  $\kappa_{sca}$  based on measured  $f(RH)$  curve by the humidified nephelometer system. The second step is predicting  $R_k$  using the look up table shown in Fig.6a, and then calculate  $\kappa_{f(RH)}$  based on predicted  $R_k$  and fitted  $\kappa_{sca}$ . The results of predicted  $\kappa_{f(RH)}$  values are shown in Fig.7b and a robust correlation between predicted- $\kappa_{f(RH)}$  values predicted from Method 4 and  $\kappa_{f(RH)}$  values derived from Method 1 retrieved by using the traditional method introduced in Sect.3.1 is achieved (the square of correlation coefficient between them is 0.99). All points shown in Fig.7b lie nearby 1:1 line, average difference between  $\kappa_{f(RH)}$  derived from newly proposed method and traditional method Method 4 and Method 1 is -0.0095. This result demonstrates a quite good estimation of  $\kappa_{f(RH)}$  can be achieved by using only measurements from a humidified nephelometer system.

Datasets from Gucheng campaign are further used to verify Method 4. In this campaign, Aurora 3000 nephelometer is used for the humidified nephelometer system, it has three wavelengths: 450 nm, 525 nm and 635 nm. Values of  $f(RH, \lambda)$  points correspond to wavelength of 525 nm are used to derive  $\kappa_{f(RH)}$  using Method 1 and Method 4, used RH range is 45% to 90%. The look up table shown in Fig.6a is simulated corresponding to scattering wavelength of 550 nm, and is not suitable for being used in Method 4 if the nephelometer is Aurora 3000. A new look up table is simulated corresponding to scattering wavelength of 525 nm, used datasets of PNSD and BC are same with those for producing the look up table shown in Fig.6a. During Gucheng campaign, the variations of  $\kappa_{f(RH)}$  and corresponding  $R_k$  with  $\sigma_{sp}$  at 525 nm are shown in Fig.8a. Values of  $\kappa_{f(RH)}$  range from 0.01 to 0.27, with an average of 0.14. During this campaign,  $\kappa_{f(RH)}$  is relatively lower when  $\sigma_{sp}$  is high. Values of  $R_k$  range from 0.60 to 0.84, with an average of 0.7. Results of the comparison between  $\kappa_{f(RH)}$  derived from Method 1 and Method 4 are shown in Fig.8b. The results demonstrate that good consistency is achieved between  $\kappa_{f(RH)}$  derived from Method 1 and Method 4, the square of correlation coefficient between them is 0.99.

The verification results of Method 4 using measurements from Wangdu and Gucheng campaigns

demonstrate that a quite good estimation of  $\kappa_{f(RH)}$  can be achieved by using only measurements from a humidified nephelometer system, and Method 4 is applicable at different sites and in different seasons.

It should be noted that the look up table shown in Fig.6a already covers large variation ranges of Ångström exponent and  $\kappa_{sca}$ . Which means that this look up table can be used under different conditions. However, it should be pointed out that the look up table shown in Fig.6a is from simulations of measured continental aerosols without influences of desert dust, and it might not be suitable for being used to estimate  $\kappa_{f(RH)}$  when sea salt or dust particles prevail. In summary, this approach allows researchers to directly derive aerosol hygroscopicity from measurements of  $f(RH)$  without any additional information about PNSD and BC which is quite convenient for researchers to conduct aerosol hygroscopicity researches with measurements from a humidified nephelometer system.

## 5. Conclusions

~~During the field campaign introduced in this paper, which is conducted in summer at a background site of the NCP, integrative aerosol information including aerosol chemical, optical and physical properties are observed. Among them, aerosol hygroscopicity is crucial for understanding roles of aerosol particles in air pollution and aerosol climate effects.~~ In this paper, values of aerosol hygroscopicity parameter  $\kappa$  during Wangdu campaign are first derived from measurements of  $f(RH)$  by combining measurements of PNSD at dry state and BC. The results show that during this field campaign, aerosol hygroscopicity varies a lot, and  $\kappa_{f(RH)}$  ranges from 0.06 to 0.5143 with an average of 0.3428. Retrieved  $\kappa_{f(RH)}$  values are further compared with  $\kappa_{250}$  which is derived from measurements of HH-TDMA and good consistency is achieved. ~~Results show that  $\kappa_{250}$  is systematically higher than  $\kappa_{f(RH)}$  and the average of their difference is 0.06. A simulative experiment is conducted to better understand their difference and partially explained the observed discrepancy, however, still not enough and possible reasons are discussed in Sect.4.1.~~

Relationships between  $\kappa_{f(RH)}$  and  $f(RH)$  fitting parameters  $\gamma$  and  $\kappa_{sca}$  are further investigated in Sect.4.2 which is for the first time to our knowledge. Good linear relationship is found exists between  $\kappa_{f(RH)}$  and  $\kappa_{sca}$  during Wangdu campaign, and the correlation between  $\kappa_{f(RH)}$  and  $\gamma$  is far better than previously found relationships between  $\gamma$  and aerosol chemical compositions. This results demonstrate that  $\kappa$  should be a better choice to parameterize  $f(RH)$  fitting parameters than mass fractions of aerosol chemical compositions which is so far widely used. The relationship

between  $\kappa_{f(RH)}$  and  $\kappa_{sea}$  is then also examined, and it is found that a better linear relationship than the relationship between  $\kappa_{f(RH)}$  and  $\gamma$  exists between  $\kappa_{f(RH)}$  and  $\kappa_{sea}$ , and  $\kappa_{f(RH)}$  may be proportional to  $\kappa_{sea}$ . However, through Results of detailed analysis about the relationship between  $\kappa_{f(RH)}$  and  $\kappa_{sea}$ , it turns out demonstrate that their relationship relationship between  $\kappa_{f(RH)}$  and  $\kappa_{sea}$  is complicated more complicated than what is found at the very beginning and, and the ratio  $\kappa_{sea}/\kappa_{f(RH)}$  ( $R_\kappa$ ) varies a lot (0.5 to 0.84, with an average of 0.69). Results show that both PNSD at dry state and aerosol hygroscopicity have impacts on value of  $R_\kappa$ .

In Sect.4.3, by introducing Ångström exponent as a proxy for PNSD, impacts of PNSD and aerosol hygroscopicity on  $R_\kappa$  are distinguished and then discussed. In succession, a look up table based on Ångström exponent and  $\kappa_{sea}$  is developed to estimate  $R_\kappa$ . With this look up table,  $R_\kappa$  as well as  $\kappa_{f(RH)}$  can be directly estimated from measurements of a humidified nephelometer system. This method is further verified with measurements of this field campaign two different campaigns. Results show that great consistency is achieved between predicted and measured  $R_\kappa$  values (92% points have relative difference less than 6%). Given this, the linkage between  $\kappa_{f(RH)}$  and  $\kappa_{sea}$  is directly established and further used to estimate  $\kappa_{f(RH)}$ . The comparison results demonstrate a pretty good agreement is achieved, all points lie nearby 1:1 line. The average absolute difference between  $\kappa_{f(RH)}$  derived from newly proposed method and traditional method is 0.005 and the square of correlation coefficient between them is 0.99. The verification results demonstrate that a quite good estimation of  $\kappa_{f(RH)}$  can be achieved by using only measurements from a humidified nephelometer system, and this method is applicable at different sites and in different seasons. This newly proposed novel approach allow researchers to estimate  $\kappa_{f(RH)}$  without any additional information about PNSD and BC. This new finding directly links  $\kappa$  and  $f(RH)$  and will make the humidified nephelometer system more convenient when it comes to aerosol hygroscopicity research. Finally, findings in this research may facilitate the intercomparison of aerosol hygroscopicity derived from different techniques, help for parameterizing  $f(RH)$  and predicting CCN properties with optical measurements.

## Acknowledgments

This work is supported by the National Natural Science Foundation of China (41590872, 41375134).

616 The data used are listed in the references and a repository at <http://pan.baidu.com/s/1c2Nzc5a>.

617

618

619

620

621 **References**

622 Anderson, T. L., and Ogren, J. A.: Determining aerosol radiative properties using the TSI 3563 integrating nephelometer,  
623 Aerosol Science and Technology, 29, 57-69, 10.1080/02786829808965551, 1998.

624 Bian, Y. X., Zhao, C. S., Ma, N., Chen, J., and Xu, W. Y.: A study of aerosol liquid water content based on hygroscopicity  
625 measurements at high relative humidity in the North China Plain, Atmos. Chem. Phys., 14, 6417-6426, 10.5194/acp-14-  
626 6417-2014, 2014.

627 Birmili, W., Stratmann, F., and Wiedensohler, A.: Design of a DMA-based size spectrometer for a large particle size range  
628 and stable operation, Journal of Aerosol Science, 30, 549-553, 10.1016/S0021-8502(98)00047-0, 1999.

629 Boucher, O., Randall, D., Artaxo, P., Bretherton, C., Feingold, G., Forster, P., Kerminen, V.-M., Kondo, Y., Liao, H., Lohmann,  
630 U., Rasch, P., Satheesh, S. K., Sherwood, S., Stevens, B., and Zhang, X. Y.: Clouds and Aerosols, in: Climate Change 2013:  
631 The Physical Science Basis. Contribution of Working Group I to the Fifth Assessment Report of the Intergovernmental  
632 Panel on Climate Change, edited by: Stocker, T. F., Qin, D., Plattner, G.-K., Tignor, M., Allen, S. K., Boschung, J., Nauels, A.,  
633 Xia, Y., Bex, V., and Midgley, P. M., Cambridge University Press, Cambridge, United Kingdom and New York, NY, USA, 571–  
634 658, 2013.

635 Brock, C. A., Wagner, N. L., Anderson, B. E., Attwood, A. R., Beyersdorf, A., Campuzano-Jost, P., Carlton, A. G., Day, D. A.,  
636 Diskin, G. S., Gordon, T. D., Jimenez, J. L., Lack, D. A., Liao, J., Markovic, M. Z., Middlebrook, A. M., Ng, N. L., Perring, A. E.,  
637 Richardson, M. S., Schwarz, J. P., Washenfelder, R. A., Welti, A., Xu, L., Ziemba, L. D., and Murphy, D. M.: Aerosol optical  
638 properties in the southeastern United States in summer – Part 1: Hygroscopic growth, Atmos. Chem. Phys., 16, 4987-5007,  
639 10.5194/acp-16-4987-2016, 2016.

640 Chen, J., Zhao, C. S., Ma, N., and Yan, P.: Aerosol hygroscopicity parameter derived from the light scattering enhancement  
641 factor measurements in the North China Plain, Atmos. Chem. Phys., 14, 8105-8118, 10.5194/acp-14-8105-2014, 2014.

642 Drinovec, L., Močnik, G., Zotter, P., Prévôt, A. S. H., Ruckstuhl, C., Coz, E., Rupakheti, M., Sciare, J., Müller, T., Wiedensohler,  
643 A., and Hansen, A. D. A.: The "dual-spot" Aethalometer: an improved measurement of aerosol black carbon with real-  
644 time loading compensation, Atmospheric Measurement Techniques, 8, 1965-1979, 10.5194/amt-8-1965-2015, 2015.

645 Ervens, B., Cubison, M. J., Andrews, E., Feingold, G., Ogren, J. A., Jimenez, J. L., Quinn, P. K., Bates, T. S., Wang, J., Zhang,  
646 Q., Coe, H., Flynn, M., and Allan, J. D.: CCN predictions using simplified assumptions of organic aerosol composition and  
647 mixing state: a synthesis from six different locations, Atmos. Chem. Phys., 10, 4795-4807, 10.5194/acp-10-4795-2010,  
648 2010.

649 Gunthe, S. S., King, S. M., Rose, D., Chen, Q., Roldin, P., Farmer, D. K., Jimenez, J. L., Artaxo, P., Andreae, M. O., Martin, S.  
650 T., and Pöschl, U.: Cloud condensation nuclei in pristine tropical rainforest air of Amazonia: size-resolved measurements  
651 and modeling of atmospheric aerosol composition and CCN activity, Atmos. Chem. Phys., 9, 7551-7575, 10.5194/acp-9-  
652 7551-2009, 2009.

653 Hänel, G.: An attempt to interpret the humidity dependencies of the aerosol extinction and scattering coefficients,  
654 Atmospheric Environment (1967), 15, 403-406, [http://dx.doi.org/10.1016/0004-6981\(81\)90045-7](http://dx.doi.org/10.1016/0004-6981(81)90045-7), 1981.

655 Hennig, T., Massling, A., Brechtel, F. J., and Wiedensohler, A.: A tandem DMA for highly temperature-stabilized hygroscopic  
656 particle growth measurements between 90% and 98% relative humidity, Journal of Aerosol Science, 36, 1210-1223,

10.1016/j.jaerosci.2005.01.005, 2005.

Kuang, Y., Zhao, C. S., Tao, J. C., and Ma, N.: Diurnal variations of aerosol optical properties in the North China Plain and their influences on the estimates of direct aerosol radiative effect, *Atmos. Chem. Phys.*, 15, 5761-5772, 10.5194/acp-15-5761-2015, 2015.

Kuang, Y., Zhao, C. S., Ma, N., Liu, H. J., Bian, Y. X., Tao, J. C., and Hu, M.: Deliquescent phenomena of ambient aerosols on the North China Plain, *Geophys. Res. Lett.*, n/a-n/a, 10.1002/2016GL070273, 2016a.

Kuang, Y., Zhao, C. S., Tao, J. C., Bian, Y. X., and Ma, N.: Impact of aerosol hygroscopic growth on the direct aerosol radiative effect in summer on North China Plain, *Atmospheric Environment*, 147, 224-233, <http://dx.doi.org/10.1016/j.atmosenv.2016.10.013>, 2016b.

Liu, H. J., Zhao, C. S., Nekat, B., Ma, N., Wiedensohler, A., van Pinxteren, D., Spindler, G., Müller, K., and Herrmann, H.: Aerosol hygroscopicity derived from size-segregated chemical composition and its parameterization in the North China Plain, *Atmos. Chem. Phys.*, 14, 2525-2539, 10.5194/acp-14-2525-2014, 2014.

Liu, P. F., Zhao, C. S., Göbel, T., Hallbauer, E., Nowak, A., Ran, L., Xu, W. Y., Deng, Z. Z., Ma, N., Mildenerberger, K., Henning, S., Stratmann, F., and Wiedensohler, A.: Hygroscopic properties of aerosol particles at high relative humidity and their diurnal variations in the North China Plain, *Atmos. Chem. Phys.*, 11, 3479-3494, 10.5194/acp-11-3479-2011, 2011.

Müller, T., Laborde, M., Kassell, G., and Wiedensohler, A.: Design and performance of a three-wavelength LED-based total scatter and backscatter integrating nephelometer, *Atmos. Meas. Tech.*, 4, 1291-1303, 10.5194/amt-4-1291-2011, 2011.

Ma, N., Zhao, C. S., Müller, T., Cheng, Y. F., Liu, P. F., Deng, Z. Z., Xu, W. Y., Ran, L., Nekat, B., van Pinxteren, D., Gnauk, T., Müller, K., Herrmann, H., Yan, P., Zhou, X. J., and Wiedensohler, A.: A new method to determine the mixing state of light absorbing carbonaceous using the measured aerosol optical properties and number size distributions, *Atmos. Chem. Phys.*, 12, 2381-2397, 10.5194/acp-12-2381-2012, 2012.

Ma, N., Zhao, C., Tao, J., Wu, Z., Kecorius, S., Wang, Z., Größ, J., Liu, H., Bian, Y., Kuang, Y., Teich, M., Spindler, G., Müller, K., van Pinxteren, D., Herrmann, H., Hu, M., and Wiedensohler, A.: Variation of CCN activity during new particle formation events in the North China Plain, *Atmos. Chem. Phys.*, 16, 8593-8607, 10.5194/acp-16-8593-2016, 2016.

Murphy, D. M., Thomson, D. S., and Mahoney, M. J.: In Situ Measurements of Organics, Meteoritic Material, Mercury, and Other Elements in Aerosols at 5 to 19 Kilometers, *Science*, 282, 1664-1669, 10.1126/science.282.5394.1664, 1998.

Petters, M. D., and Kreidenweis, S. M.: A single parameter representation of hygroscopic growth and cloud condensation nucleus activity, *Atmospheric Chemistry and Physics*, 7, 1961-1971, 2007.

Petters, M. D., Carrico, C. M., Kreidenweis, S. M., Prenni, A. J., DeMott, P. J., Collett, J. L., and Moosmüller, H.: Cloud condensation nucleation activity of biomass burning aerosol, *Journal of Geophysical Research: Atmospheres*, 114, n/a-n/a, 10.1029/2009JD012353, 2009.

Pinnick, R. G., Jennings, S. G., and Chýlek, P.: Relationships between extinction, absorption, backscattering, and mass content of sulfuric acid aerosols, *Journal of Geophysical Research: Oceans*, 85, 4059-4066, 10.1029/JC085iC07p04059, 1980.

Quinn, P. K., Bates, T. S., Baynard, T., Clarke, A. D., Onasch, T. B., Wang, W., Rood, M. J., Andrews, E., Allan, J., Carrico, C. M., Coffman, D., and Worsnop, D.: Impact of particulate organic matter on the relative humidity dependence of light scattering: A simplified parameterization, *Geophys. Res. Lett.*, 32, n/a-n/a, 10.1029/2005GL024322, 2005.

Rose, D., Nowak, A., Achtert, P., Wiedensohler, A., Hu, M., Shao, M., Zhang, Y., Andreae, M. O., and Pöschl, U.: Cloud condensation nuclei in polluted air and biomass burning smoke near the mega-city Guangzhou, China – Part 1: Size-resolved measurements and implications for the modeling of aerosol particle hygroscopicity and CCN activity, *Atmos. Chem. Phys.*, 10, 3365-3383, 10.5194/acp-10-3365-2010, 2010.

Seinfeld, J. H., and Pandis, S. N.: *Atmospheric chemistry and physics: from air pollution to climate change*, John Wiley & Sons, 2006.

Su, H., Rose, D., Cheng, Y. F., Gunthe, S. S., Massling, A., Stock, M., Wiedensohler, A., Andreae, M. O., and Pöschl, U.:

Hygroscopicity distribution concept for measurement data analysis and modeling of aerosol particle mixing state with regard to hygroscopic growth and CCN activation, *Atmos. Chem. Phys.*, 10, 7489-7503, 10.5194/acp-10-7489-2010, 2010.

Tao, J. C., Zhao, C. S., Ma, N., and Liu, P. F.: The impact of aerosol hygroscopic growth on the single-scattering albedo and its application on the NO<sub>2</sub> photolysis rate coefficient, *Atmos. Chem. Phys.*, 14, 12055-12067, 10.5194/acp-14-12055-2014, 2014.

Titos, G., Lyamani, H., Cazorla, A., Sorribas, M., Foyo-Moreno, I., Wiedensohler, A., and Alados-Arboledas, L.: Study of the relative humidity dependence of aerosol light-scattering in southern Spain, *Tellus Ser. B-Chem. Phys. Meteorol.*, 66, 15, 10.3402/tellusb.v66.24536, 2014.

Titos, G., Cazorla, A., Zieger, P., Andrews, E., Lyamani, H., Granados-Muñoz, M. J., Olmo, F. J., and Alados-Arboledas, L.: Effect of hygroscopic growth on the aerosol light-scattering coefficient: A review of measurements, techniques and error sources, *Atmospheric Environment*, 141, 494-507, <http://dx.doi.org/10.1016/j.atmosenv.2016.07.021>, 2016.

Wex, H., Neususs, C., Wendisch, M., Stratmann, F., Koziar, C., Keil, A., Wiedensohler, A., and Ebert, M.: Particle scattering, backscattering, and absorption coefficients: An in situ closure and sensitivity study, *Journal of Geophysical Research-Atmospheres*, 107, 18, 10.1029/2000jd000234, 2002.

Wu, Z. J., Zheng, J., Shang, D. J., Du, Z. F., Wu, Y. S., Zeng, L. M., Wiedensohler, A., and Hu, M.: Particle hygroscopicity and its link to chemical composition in the urban atmosphere of Beijing, China, during summertime, *Atmos. Chem. Phys.*, 16, 1123-1138, 10.5194/acp-16-1123-2016, 2016.

You, Y., Smith, M. L., Song, M., Martin, S. T., and Bertram, A. K.: Liquid-liquid phase separation in atmospherically relevant particles consisting of organic species and inorganic salts, *International Reviews in Physical Chemistry*, 33, 43-77, 10.1080/0144235X.2014.890786, 2014.

Zhang, L., Sun, J. Y., Shen, X. J., Zhang, Y. M., Che, H., Ma, Q. L., Zhang, Y. W., Zhang, X. Y., and Ogren, J. A.: Observations of relative humidity effects on aerosol light scattering in the Yangtze River Delta of China, *Atmos. Chem. Phys.*, 15, 8439-8454, 10.5194/acp-15-8439-2015, 2015.

Zhao, C., Tie, X., and Lin, Y.: A possible positive feedback of reduction of precipitation and increase in aerosols over eastern central China, *Geophys. Res. Lett.*, 33, L11814, 10.1029/2006GL025959, 2006.

Zieger, P., Fierz-Schmidhauser, R., Weingartner, E., and Baltensperger, U.: Effects of relative humidity on aerosol light scattering: results from different European sites, *Atmos. Chem. Phys.*, 13, 10609-10631, 10.5194/acp-13-10609-2013, 2013.

Zieger, P., Fierz-Schmidhauser, R., Poulain, L., Muller, T., Birmili, W., Spindler, G., Wiedensohler, A., Baltensperger, U., and Weingartner, E.: Influence of water uptake on the aerosol particle light scattering coefficients of the Central European aerosol, *Tellus Ser. B-Chem. Phys. Meteorol.*, 66, 10.3402/tellusb.v66.22716, 2014.

745  
746  
747  
748  
749  
750  
751  
752  
  
753  
754  
755  
756  
757  
758  
759  
760  
761  
762  
763  
764  
765

**Table 1.** Locations, time periods and used datasets of five field campaigns

Location	Wuqing	Wuqing	Xianghe	Wangdu	Gucheng
Time period	7 march to 4 April, 2009	12 July to 14 August, 2009	9 July to 8 August, 2013	4 June to 14 July, 2014	15 October to 25 November, 2016
PNSD	TSMPS+APS	TSMPS+APS	TSMPS+APS	TSMPS+APS	SMPS+APS
BC	MAAP	MAAP	MAAP	MAAP	AE33
$\sigma_{sp}$	TSI 3563	TSI 3563	TSI 3563	TSI 3563	Aurora 3000
$f(RH)$				Humidified nephelometer system	Humidified nephelometer system
$g(RH)$				HH-TDMA	



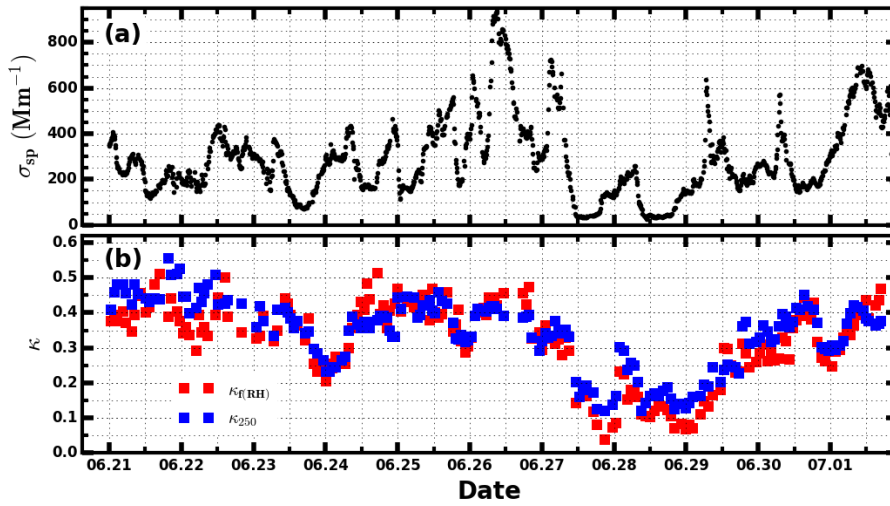


**Figure 1.** (a) The time series of  $\sigma_{sp}$  at 550 nm; (b) The time series of  $\kappa$  values derived from  $f(RH)$  measurements ( $\kappa_{f(RH)}$ ) by combining information of PNSD and BC, and time series of average  $\kappa$  values of aerosol particles at 250 nm ( $\kappa_{250}$ ) which is calculated from measurements of HH-TDMA.

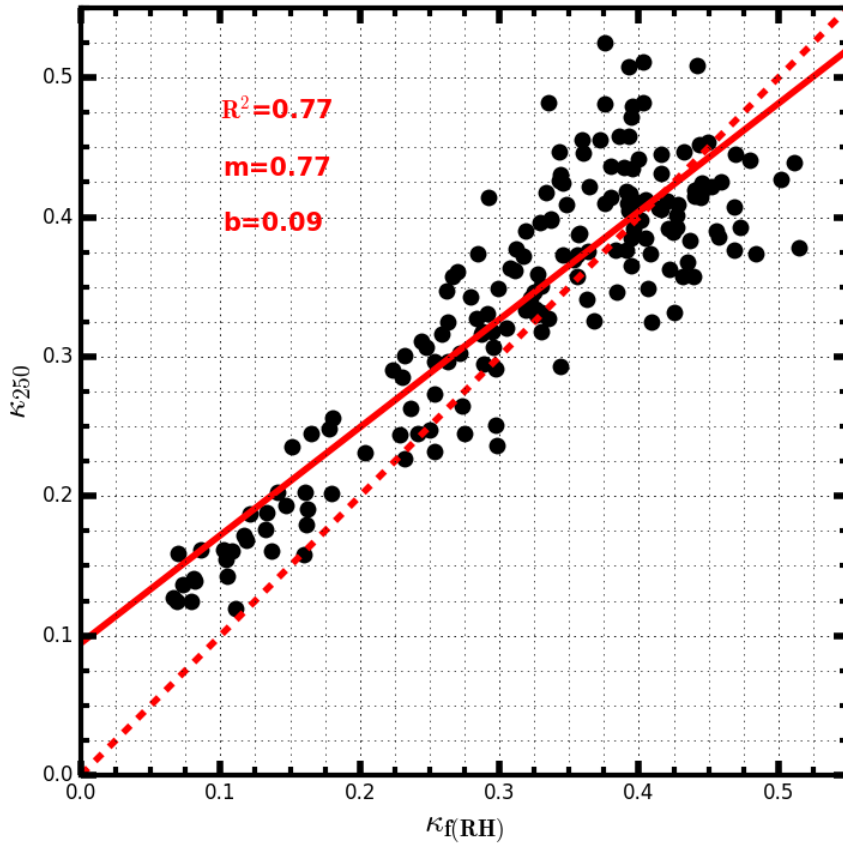


**Figure 2.** The comparison between  $\kappa$  values derived from  $f(RH)$  measurements ( $\kappa_{f(RH)}$ ) and average  $\kappa$  values for aerosol particles with a diameter of 250 nm ( $\kappa_{250}$ ) which are derived from measurements of HH-TDMA.  $R^2$  is the square of correlation coefficient,  $m$  is the slope and  $b$  is the intercept.

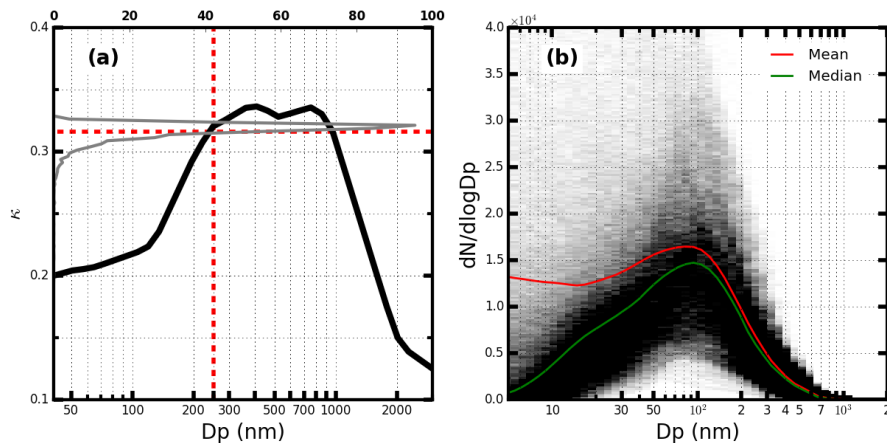


**Figure 3.** (a) The thick black line represents the average size-resolved  $\kappa$  distribution from HaChi campaign. The solid gray line represents the probability distribution of retrieved  $\kappa$  values with this size-resolve  $\kappa$  distribution by using all PNSDs shown in figure (b), and the horizontal dashed line represents their average. The vertical dashed red line represents the position of 250 nm. (b) All PNSDs which are observed from three different representative background sites of the NCP during summer, they are used to model relationship between size-resolved  $\kappa$  and retrieved  $\kappa$  values from  $f(\text{RH})$  measurements, and the gray color represents the frequency of PNSD, darker point corresponds to higher frequency, red and green line represent mean of median values of all observed PNSDs.

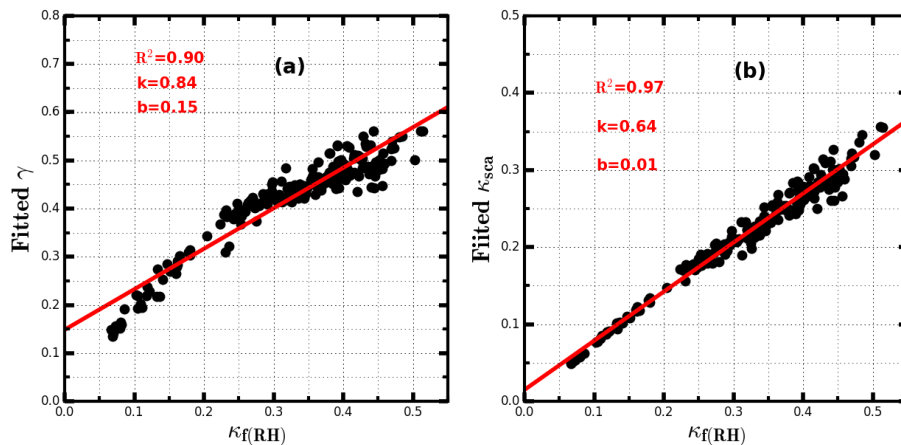
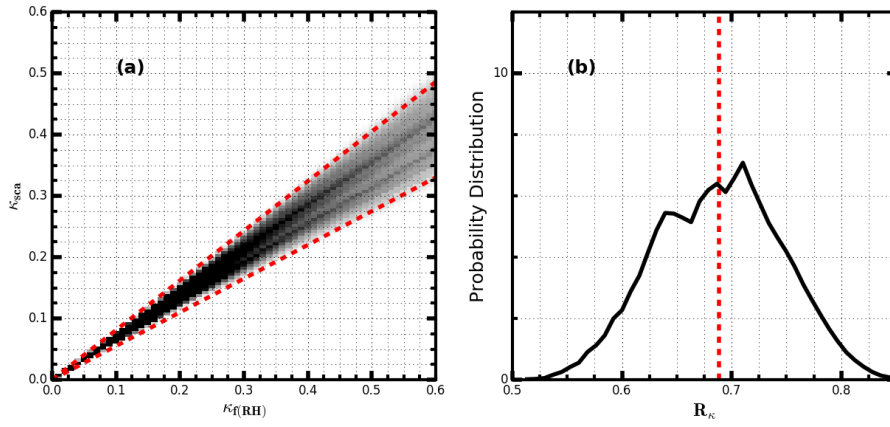


**Figure 4.** (A) Fitting example of two discussed parameterization schemes, and title shows the observation time of this  $f(\text{RH})$  curve; (B) The fitting performance of two discussed parameterization schemes, x-axis represents the ratio between fitted  $f(85\%)$  and measured  $f(85\%)$  and y-axis represents the probability distribution. (aC) The linear relationship between values of  $\kappa_{f(\text{RH})}$  and fitted  $\gamma$ ,  $R^2$  is the square of correlation coefficient, k is the slope and b is the intercept; (bD) The linear relationship between values of  $\kappa_{f(\text{RH})}$  and fitted  $\kappa_{\text{sca}}$ .

796  
797  
798  
799  
800  
801



802  
803  
804  
805  
806  
807  
808  
809  
810  
811  
812  
813  
814  
815  
816  
817

**Figure 5.** (a) Simulated relationships between  $\kappa_{f(RH)}$  and  $\kappa_{sca}$  under different PNSD conditions ( all PNSDs shown in Fig.3a are used as inputs to conduct the simulation experiment), gray color represents the frequency and darker point corresponds to higher frequency, the slope of two dashed lines are 0.55 and 0.81; (b) The probability distribution of  $R_{\kappa}$  ( $\kappa_{sca}/\kappa_{f(RH)}$ ).

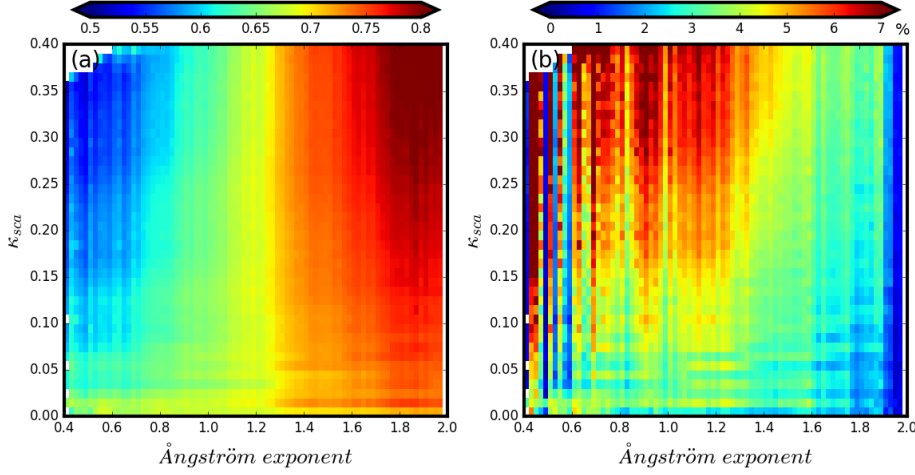


**Figure 6.** (a) Colors represent  $R_\kappa$  values and the color bar is shown on the top of this figure, x-axis represents Ångström exponent and y-axis represents  $\kappa_{sca}$ . (b) Meanings of x-axis and y-axis are same with them in (a), however, color represents the percentile value of the standard deviation of  $R_\kappa$  values within each grid divided by their average.

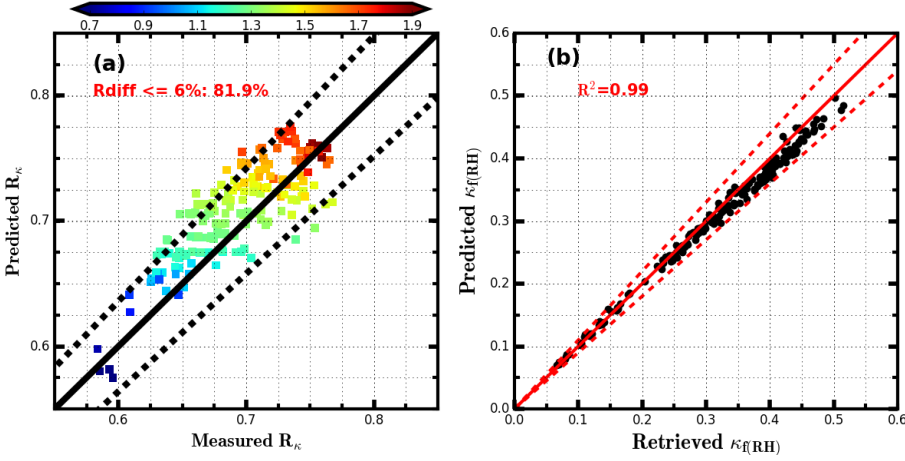
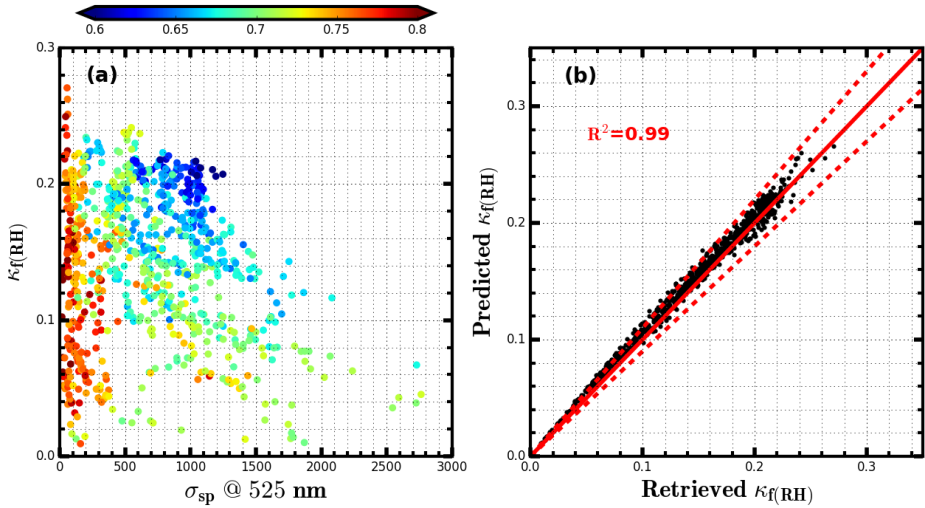


**Figure 7.** (a) The comparison between measured and predicted  $R_\kappa$  values, colors represent values of Ångström exponent, texts with red color show the percentile of points with relative difference (Rdiff) less than 6%, two dashed line are 6% relative difference lines with absolute relative difference (Rdiff) equal to 6%; (b) the comparison between retrieved  $\kappa_f(RH)$  values by using traditional method introduced in Sect.3.1 retrieved from Method 1 and predicted  $\kappa_f(RH)$  by using the new method introduced in Sect.4.3,  $R^2$  is the square of correlation coefficient, two dashed lines

831 are 10% relative difference lines.  $k$  is the slope and  $b$  is the intercept.  
832



833  
834 **Figure 8.** (a) x axis represents  $\sigma_{sp}$  at 525 nm ( $Mm^{-1}$ ), y axis represents retrieved  $\kappa_{f(RH)}$ , colors of scatter points  
835 represent corresponding values of  $R_K$ ; (b) The comparison between  $\kappa_{f(RH)}$  retrieved from Method 1 and predicted  
836  $\kappa_{f(RH)}$  by using the new method,  $R^2$  is the square of correlation coefficient, two dashed red lines represent 10%  
837 deviations from 1:1 line.

带格式的：正文

带格式的：与下段同页

带格式的：字体：加粗

带格式的：字体：（默认）Times New Roman，五号

带格式的：字体：（默认）+西文标题（Calibri Light），  
10 磅